Anomalous dimensions and critical exponents for the Gross-Neveu-Yukawa model at five loops

J.A. Gracey*
Theoretical Physics Division, Department of Mathematical Sciences, University of Liverpool, Liverpool, L69 3BX, United Kingdom

A. Maier†
Institut de Física d'Altes Energies (IFAE), The Barcelona Institute of Science and Technology, Campus UAB, 08193 Bellaterra (Barcelona), Spain and Grup de Física Teòrica, Dept. Física, Universitat Autònoma de Barcelona, E-08193 Bellaterra, Barcelona, Spain

P. Marquard‡
Deutsches Elektronen–Synchrotron DESY, Platanenallee 6, 15738 Zeuthen, Germany

Y. Schröder§
Centro de Ciencias Exactas, Departamento de Ciencias Básicas, Universidad del Bío-Bío, Avenida Andrés Bello 720, Chillán, Chile

We renormalize the Gross-Neveu-Yukawa model with an $O(N)$ symmetry to $\mathcal{O}(\epsilon^5)$ in $d = 4 - \epsilon$ dimensions and determine the anomalous dimensions of the fermion and scalar fields, β-functions as well as the scalar field's mass operator. These are used to construct several N dependent critical exponents relevant for quantum transitions in semi-metals and in particular those connected with graphene in three dimensions when $N = 2$. Improved exponent estimates for scalar fermion transitions on a honeycomb lattice, when $N = 1$, as well as for $N = 5$ are also given to compare with results from other techniques such as the conformal bootstrap.

I. INTRODUCTION

Wilson's development of the renormalization group equation led to a beneficial and practical tool to study critical phenomena with applications to phase transitions seen in Nature, [1]. In particular continuum analytic quantum field theory techniques could be used alongside numerical methods employed in discrete models to study critical points in the renormalization group flow. The ultimate goal being to estimate the observables which are the critical exponents. If determined accurately enough the exponents could be tested against experimental values and thereby confirm symmetry properties of the phase transition that are intrinsic to the underlying continuum or discrete field theory.

One of the more widely known applications of the critical renormalization group equation is that of transitions in the three dimensional Heisenberg ferromagnet where critical exponents are available at very high precision from techniques such as perturbation theory, Monte Carlo methods, functional renormalization group together with the recent incarnation of the conformal bootstrap summarized in [2] for instance. The latter method, for example, has generally produced exponents to the highest numerical precision. It is founded on exploiting the conformal symmetry inherent at a fixed point to determine the scaling behaviour of field and operator correlation functions. See [3], for example, for a comprehensive overview of the current conformal field theory properties of the scalar field theories underlying the Heisenberg ferromagnet transition.

One key principle of the study of critical phenomena is that seemingly different models used to understand, say the Heisenberg example, are related in that they lie in the same universality class of the core fixed point. In this Heisenberg case the three dimensional fixed point is the Wilson-Fisher one, [4], corresponding to the non-trivial critical point of the underlying field theory. It is known that continuum scalar ϕ^4 theory is one of the members of this universality class. Although its critical dimension is four it is still possible to derive exponent estimates in three dimensions. Indeed as the available loop order of ϕ^4 theory renormalization group functions increase, [5–7], there have been several resummation studies based on the ϵ expansion.

However a second continuum field theory is believed to be present in the same universality class which is the nonlinear σ model whose critical dimension is two. In fact there is in principle an infinite tower of theories in even

* gracey@liverpool.ac.uk
† amaier@ifae.es
‡ peter.marquard@desy.de
§ yschroder@ubiobio.cl

spacetime dimensions which reside in the same class. What they share in common across all dimensions is the same core interaction with additional spectator interactions included in specific dimensions to ensure renormalizability and therefore calculability. This concept of tower is not unrelated to the notion of ultraviolet completion.

Although this instance of connecting critical theories across dimensions to extract precision estimates for observables is well-known it is not an isolated case with physical applications. In more recent years a second main universality class has emerged which is connected to transitions in recently developed materials. Perhaps the best known example is that of critical phenomena in graphene. This is a one atom thick sheet of carbon atoms connected at the corners of a hexagonal lattice. Stretching a sheet of graphene can change its electrical properties and it is believed the critical properties of the transition from having semi-metal properties to becoming an insulator is described by a resident theory of what is termed the Gross-Neveu (GN) or Gross-Neveu-Yukawa (GNY) universality class. The two main continuum field theories connected with the class are the two dimensional Gross-Neveu model, [8], and the four dimensional Gross-Neveu-Yukawa theory, [9]. Both theories involve an $O(N)$ multiplet of Dirac fermions coupled to a scalar field. In two dimensions the scalar is an auxiliary field, [8], and the GN model reverts to a quartic fermion interaction. In the GNY model an extra quartic scalar interaction is required as a spectator interaction to ensure renormalizability.

Unlike the purely scalar field theory universality class of the Heisenberg model the GNY class is more extensive. This is because the core scalar-Yukawa interaction can be adapted to include spin-related features as well as different fermion species. Moreover it is not unrelated to the Standard Model of particle physics which has the same underlying interactions but decorated with a more intricate general symmetry group. Indeed the GNY model offers itself as a potential laboratory to test possible beyond the standard model ideas. For instance, in [10–13] it was observed that for Lagrangians with certain field content critical points can emerge with symmetries that are not present in the original Lagrangian. In particular supersymmetry can actually emerge in a variety of theories within the broad GNY universality class at fixed points where the two critical couplings are equivalent. Moreover the scalar and fermion anomalous dimension exponents become equal at criticality. For example, see [14] for an in-depth discussion.

Since the turn of the century there has been intense activity to produce numerically precise exponent estimates for the GNY universality class with the graphene example of $N = 2$ being the primary goal with the connection having been established in [15, 16]. Other values of N are also studied as they relate to transitions in other materials. A variety of techniques have been applied such as Monte Carlo or lattice field theory, [17–24], functional renormalization group, [25–27], conformal bootstrap, [28–30], $1/N$ expansion, [31–36], and continuum perturbation theory, [37–40]. While different approximations will not always produce exact agreement of exponents, it is generally the case that the computational direction of travel in recent years is leading towards a consensual picture. Indeed the most recent conformal bootstrap analysis of [29, 30] has produced the most accurate, with respect to small uncertainties, numerical estimates for the graphene transition.

One of the other main continuum field theory approaches is that of perturbation theory with calculations to four loops being carried out in the GNY class in four dimensions in [9, 38–41] as well as in the generalization of that class recently recorded in [42]. Coupled with the parallel results to four loops in the GN model of [8, 37, 43–47] the authors of [40] produced a set of three dimensional exponent estimates based on the full four loop universality class data using several resummation techniques.

With the subsequent advance made in conformal bootstrap technology, [29, 30], it is therefore the purpose of this article to advance the perturbative information for the GNY theory to *five* loops. This is not a trivial exercise since it is beset with a significant increase in the number of Feynman graphs to compute at this order driven by the presence of two interactions.

Having established all the relevant renormalization group functions at this new order, the second phase of our investigation is to refine the four loop exponent estimates of [40]. We achieve this by employing two resummation methods that on the whole produce numerical values that are generally mutually compatible with the more recent conformal bootstrap values. Our summation methods will allow us to construct an approximation to the d-dimensional structure of the respective exponents between two and four dimensions from which we extract their values in three dimensions.

While the graphene application has clearly more general interest, we will consider other values of N. For instance in the GNY class the $N = 1$ critical exponents describe the semi-metal to insulator transition for a spinless system. Although previous activity on this substance is not as extensive as that of graphene, we find a degree of convergence of the perturbative estimates as well as consensual agreement with other techniques. However in order to try and understand some of the subtleties of our resummation analysis the case of $N = 5$ is also considered for comparison with other approaches. Indeed it appears that exponent estimates in the general GNY class do agree more precisely as N increases hinting that the situation with lower N exponents would perhaps stabilize were higher loop order data available.

The article is organized as follows. We describe the salient aspects of the underlying GNY theory Lagrangian in Section II including our conventions and Feynman rules before summarizing the technicalities behind the extension of

previous results to five loops. The outcome of our computations is recorded in Section III where the two β-functions and field anomalous dimensions are presented as well as the anomalous dimension of the scalar field mass operator. As a derivative goal of the five loop work is to establish critical exponents estimates for three dimensional materials we discuss the derivation of the ϵ expansion for the relevant ones in Section IV. Section V is devoted to establishing and analysing exponent estimates for several values of N using two main resummation methods as well as a comparison of where these new values sit in relation to results from non-perturbation theory techniques. Concluding remarks are provided in Section VI ahead of Appendix A and B. The former Appendix details the non-trivial consistency check of the perturbative ϵ expansion of the exponents of Sections III and IV with the same expansion of the exponents evaluated in the large N approximation. The latter Appendix records the four loop ϵ expansion of the GN model exponents in the same conventions used in this article.

II. GNY MODEL AND METHOD

We begin by recalling the structure of the basic GNY theory that we renormalize at five loops. The Lagrangian in $d = 4 - \epsilon$ Euclidean spacetime dimensions expressed in terms of renormalized quantities is

$$\mathcal{L} = Z_\psi \bar{\psi} \partial\!\!\!/ \psi + Z_{\phi\bar{\psi}\psi} y \mu^{\frac{\epsilon}{2}} \phi \bar{\psi} \psi + \frac{1}{2} \phi (Z_{\phi^2} m^2 - Z_\phi \partial_i^2) \phi + Z_{\phi^4} \lambda \mu^\epsilon \phi^4, \tag{1}$$

where ϕ is a real scalar and ψ a multiplet of N Dirac fermions. For orientation with other perturbative computations in the GNY model we will follow the notation used in [39]. As we will employ dimensional regularization throughout the scale μ is introduced to ensure the coupling constants y and λ are dimensionless in the regularized Lagrangian. Aside from the underlying $O(N)$ symmetry of the fermion multiplet the Lagrangian possesses a discrete chiral symmetry

$$\psi \ \to \gamma^5 \psi \quad , \quad \bar{\psi} \ \to - \bar{\psi} \gamma^5 \ . \tag{2}$$

We use the short-hand notation $q\!\!\!/ = q_i \gamma_i$ with four-dimensional Euclidean Dirac matrices fulfilling $\{\gamma_i, \gamma_j\} = 2\delta_{ij} \mathbb{1}_4$. Treating the boson mass m as a small perturbation we obtain the following Feynman rules:

$Z_\psi \times$ 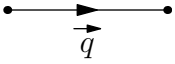 $= - i \dfrac{q\!\!\!/}{q^2}$, (3)

$Z_\phi \times$ 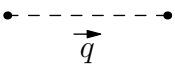 $= \dfrac{1}{q^2}$, (4)

 $= - Z_{\phi^2} m^2$, (5)

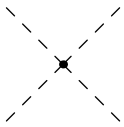 $= - 4! Z_{\phi^4} \lambda \mu^\epsilon$, (6)

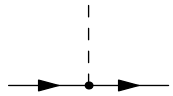 $= - Z_{\phi\bar{\psi}\psi} g \mu^{\frac{\epsilon}{2}}$. (7)

To determine the four renormalization constants Z_ψ, Z_ϕ, Z_{ϕ^4} and $Z_{\phi\bar{\psi}\psi}$ we respectively consider the fermion and boson self-energies, the truncated four-boson vertex and the truncated fermion-boson vertex. The remaining renormalization constant, Z_{ϕ^2}, is extracted from the $\mathcal{O}(m^2)$ contributions to the boson propagator, setting $m = 0$ everywhere else. We use `QGRAF` [48] to generate the Feynman diagrams to five-loop order.

The subsequent stage is to isolate the ultraviolet divergences by introducing an auxiliary mass M [49–51], which is independent of the boson mass m. This is achieved by adding a term $\frac{1}{2} Z_{M^2} M^2 \phi^2$ to the Lagrangian in equation (1). Next, we turn the Feynman rules for the propagators $\mathcal{D}$, c.f. equations (3) and (4), into iterative equations of the form

$$\mathcal{D} = \mathcal{D}_0 (1 - \mathcal{D}_0^{-1} \delta Z \mathcal{D}), \tag{8}$$

where $\mathcal{D}_0 = Z\mathcal{D}$ is the bare tree-level propagator and $\delta Z = Z - 1$. We then introduce the auxiliary mass M in the denominator of the $\mathcal{D}_0$ prefactor. The resulting propagator Feynman rules read:

$$\mathcal{D}_\psi \equiv \quad = -i\frac{\not{q}}{q^2+M^2}(1 - i\delta Z_\psi \not{q}\mathcal{D}_\psi), \tag{9}$$

$$\mathcal{D}_\phi \equiv \quad = \frac{1}{q^2+M^2}(1 - q^2\delta Z_\phi \mathcal{D}_\phi - M^2 Z_{M^2}\mathcal{D}_\phi). \tag{10}$$

With this we expand the fermion self-energy to linear order in the external momentum and the $\mathcal{O}(m^0)$ contributions to the boson self-energy to quadratic order. In the $\mathcal{O}(m^2)$ contributions and in the vertices we directly set the external momenta to zero.

With two mass scales, m and M one might, in principle, expect tadpole contributions to arise. While they are scaleless in the original formulation with $m \to 0$, this is no longer the case after introducing the auxiliary mass M. However, the sum of degrees of all vertices forming a tadpole has to be odd, implying that the number of boson-fermion vertices is odd. Since all fermion loops inside the tadpole are closed, at least one of them has an odd number of fermion propagators. As the auxiliary mass only occurs in the denominators of the fermion propagators, the trace for this loop and therefore the whole tadpole vanishes.

Having summarized the algorithm that produces infrared regularized Feynman graphs, we use `FORM` [52, 53] to insert the Feynman rules and expand the integrals in the external momentum. With the help of custom code [54] based on `nauty` and `Traces` [55] we identify the resulting 3425333 scalar integrals with four five-loop integral families of massive vacuum diagrams, depicted in Figure 1.

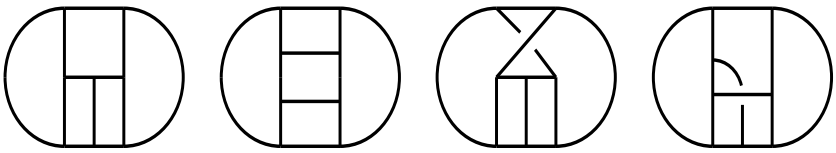

FIG. 1. There are four distinct fully massive five-loop vacuum-type integral sectors with 12 propagators. All our integrals can be mapped onto these (or their sub-sectors that result after contracting a subset of propagator lines) after performing the infrared regularization as explained in the text.

To reduce the scalar integrals to a small set of 110 basis integrals we use Laporta's algorithm [56] as implemented in our custom codes `crusher` [57] and `tinbox` [58]. Exploiting integration-by-parts identities [59, 60], we obtain large systems of linear equations, which we solve via finite-field reconstruction techniques [61–65].

To complete the reduction and map all results onto the minimal set of 110 fully massive vacuum master integrals, we employ another in-house code `Spades` [66] which is again based on integration by parts relations and the Laporta algorithm. This set of 5-loop masters had been evaluated previously to very high numerical precision [66–68], using difference equations [56] and employing Fermat [69] for fast polynomial algebra. The corresponding numerical results satisfy a large number of internal consistency checks, and have already contributed to various projects [70–73] and hence can be regarded as reliable. We note once more that, although our high-precision numerical results exclude the 12-propagator top-level families shown in Figure 1, for the renormalization constants those contribute only in three particular linear combinations. It had been observed before that those combinations can be fixed by requiring consistent pole cancellations in renormalization as well as the absence of certain combinations of group factors, as explained in detail in [71]; see also [72]. The same mechanism is at play in our present calculation, such that we can finally employ PSLQ [74] and express all our results in terms of zeta values only.

We close this section by recalling the connection of (1) with the GN model of [8] which has the two dimensional Euclidean Lagrangian

$$\mathcal{L}^{\rm GN} \;=\; \bar{\psi}\partial\!\!\!/\psi \;+\; h\phi\bar{\psi}\psi \;+\; \frac{1}{2}\phi^2 \tag{11}$$

where h is the coupling constant. Renormalization constants have been suppressed to avoid confusion with those of the four dimensional Lagrangian. The ϕ field now plays the role of an auxiliary field in two dimensions. Eliminating it from (11) produces a quartic fermion interaction leading to an asympotically free theory. However it is the shared scalar-Yukawa interaction of (1) and (11) that drives the Wilson-Fisher critical point equivalence of both theories between two and four dimensions. The GN Lagrangian also obeys the same discrete chiral symmetry as (2).

III. RESULTS

Having described the field theory side of our computation to effect the full five loop renormalization we record the results of our mammoth calculation in this section. The five renormalization constants are translated into the renormalization group functions using standard methods and our expressions have been determined in the $\overline{\rm MS}$ scheme.

A. β functions

First we record the two β-functions which are defined by

$$\beta_\lambda(\lambda,y) \;=\; \frac{d\lambda}{d\ln\mu}, \quad \beta_y(\lambda,y) \;=\; \frac{dy}{d\ln\mu} \tag{12}$$

and we will suppress the arguments λ and y throughout this section. To ease the presentation of the results we have chosen to give the coefficients of each loop order separately by defining

$$\beta_y = -\epsilon y + \sum_{L=1}^{5} \beta_y^{(L)}, \quad \beta_\lambda = -\epsilon\lambda + \sum_{L=1}^{5} \beta_\lambda^{(L)} \tag{13}$$

where the ϵ terms reflect the dimensionlessness of the coupling constants in the regularized theory. For β_λ we have

$$\begin{aligned}
\beta_\lambda^{(1)} &= 36\lambda^2 + 4\lambda Ny - Ny^2 \\
\beta_\lambda^{(2)} &= -816\lambda^3 - 72\lambda^2 Ny + 7\lambda Ny^2 + 4Ny^3 \\
\beta_\lambda^{(3)} &= 216\left(96\zeta_3 + 145\right)\lambda^4 + 1548\lambda^3 Ny - 108\lambda^2 N^2y^2 + \frac{3}{2}\left(648\zeta_3 + 361\right)\lambda^2 Ny^2 + \frac{217}{2}\lambda N^2y^3 \\
&\quad -\frac{3}{16}\left(624\zeta_3 + 1465\right)\lambda Ny^3 - \frac{157}{8}N^2y^4 + \left(\frac{5}{32} - 12\zeta_3\right)Ny^4 \\
\beta_\lambda^{(4)} &= 432\left(864\zeta_4 - \left(3744\zeta_3 + 5760\zeta_5 + 3499\right)\right)\lambda^5 + 36\left(1728\zeta_4 - 3456\zeta_3 - 1355\right)\lambda^4 Ny + 24\left(72\zeta_3 + 263\right)\lambda^3 N^2y^2 \\
&\quad -4\left(5184\zeta_4 + 7452\zeta_3 + 17280\zeta_5 + 14521\right)\lambda^3 Ny^2 + 144\left(2\zeta_3 - 1\right)\lambda^2 N^3y^3 \\
&\quad + \left(1944\zeta_4 - 4392\zeta_3 - \frac{15649}{2}\right)\lambda^2 N^2y^3 + \left(2511\zeta_4 + 456\zeta_3 + 10440\zeta_5 + \frac{211565}{16}\right)\lambda^2 Ny^3 \\
&\quad + \left(\frac{1685}{12} - 228\zeta_3\right)\lambda N^3y^4 + \left(-675\zeta_4 + 1039\zeta_3 - 840\zeta_5 + \frac{17305}{12}\right)\lambda N^2y^4 \\
&\quad + \left(-\frac{123}{2}\zeta_4 + \frac{4677\zeta_3}{4} + 785\zeta_5 + \frac{9745}{16}\right)\lambda Ny^4 + \left(42\zeta_3 - \frac{193}{6}\right)N^3y^5 + \left(24\zeta_4 - 45\zeta_3 + 160\zeta_5 + \frac{1289}{12}\right)N^2y^5 \\
&\quad + \left(-\frac{231}{8}\zeta_4 + \frac{277\zeta_3}{4} + \frac{325\zeta_5}{4} - \frac{4473}{128}\right)Ny^5 \\
\beta_\lambda^{(5)} &= -108\left(777600\zeta_6 + 342432\zeta_4 - \left(103680{\zeta_3}^2 + 1146960\zeta_3 + 2274048\zeta_5 + 3048192\zeta_7 + 764621\right)\right)\lambda^6 \\
&\quad -18\left(691200\zeta_6 + 404352\zeta_4 + 110592{\zeta_3}^2 - 499824\zeta_3 - 1340928\zeta_5 - 78653\right)\lambda^5 Ny \\
&\quad -\frac{27}{2}\left(23328\zeta_4 + 8352\zeta_3 + 4608\zeta_5 + 29969\right)\lambda^4 N^2y^2 + \left(3888\zeta_4 - 22824\zeta_3 + 9609\right)\lambda^3 N^3y^3 \\
&\quad + \left(3110400\zeta_6 + 1560060\zeta_4 + 2363904{\zeta_3}^2 + 3048516\zeta_3 + 301968\zeta_5 + 9344160\zeta_7 + \frac{19945539}{4}\right)\lambda^4 Ny^2 \\
&\quad + \left(-259200\zeta_6 + 27702\zeta_4 - 62208{\zeta_3}^2 + 378954\zeta_3 + 662256\zeta_5 + \frac{993027}{2}\right)\lambda^3 N^2y^3 \\
&\quad + \left(-129600\zeta_6 - 8127\zeta_4 - 67392{\zeta_3}^2 - 414546\zeta_3 - 115176\zeta_5 - 1714608\zeta_7 - \frac{5584765}{8}\right)\lambda^3 Ny^3 \\
&\quad +36\left(15\zeta_4 - 10\zeta_3 - 5\right)\lambda^2 N^4y^4 + \left(-7182\zeta_4 + 18243\zeta_3 + 3060\zeta_5 - \frac{124691}{8}\right)\lambda^2 N^3y^4 \\
&\quad + \left(106875\zeta_6 + \frac{3393\zeta_4}{4} + 36054{\zeta_3}^2 - \frac{88791\zeta_3}{4} - 165711\zeta_5 + 77868\zeta_7 - \frac{8026377}{128}\right)\lambda^2 N^2y^4
\end{aligned}$$

$$
\begin{aligned}
&+\left(\frac{82125\zeta_6}{4}-\frac{218691\zeta_4}{16}+\frac{9837{\zeta_3}^2}{2}-\frac{505953\zeta_3}{16}-57432\zeta_5-\frac{969381\zeta_7}{8}-\frac{13919569}{256}\right)\lambda^2Ny^4\\
&+\left(-450\zeta_4+248\zeta_3+\frac{699}{4}\right)\lambda N^4y^5+\left(-2100\zeta_6+\frac{17379\zeta_4}{8}-408{\zeta_3}^2-\frac{20021\zeta_3}{8}+3328\zeta_5+\frac{1349851}{192}\right)\lambda N^3y^5\\
&+\left(-\frac{44725\zeta_6}{4}+\frac{12801\zeta_4}{2}-\frac{1469{\zeta_3}^2}{2}-9906\zeta_3+\frac{24515\zeta_5}{2}-16233\zeta_7-\frac{14188555}{768}\right)\lambda N^2y^5\\
&+\left(1250\zeta_6+\frac{30249\zeta_4}{16}+\frac{1}{512}\left(-1533056{\zeta_3}^2-4967520\zeta_3-4893984\zeta_5-2564016\zeta_7+538157\right)\right)\lambda Ny^5\\
&+\left(90\zeta_4-\frac{157\zeta_3}{4}-\frac{2623}{64}\right)N^4y^6+\left(\frac{1125\zeta_6}{2}-\frac{603\zeta_4}{4}+87{\zeta_3}^2-\frac{1287\zeta_3}{8}-899\zeta_5-\frac{342865}{384}\right)N^3y^6\\
&+\left(\frac{18925\zeta_6}{32}-\frac{25245\zeta_4}{64}+\frac{-358464{\zeta_3}^2-343920\zeta_3-4913088\zeta_5-1495872\zeta_7+901799}{3072}\right)N^2y^6\\
&+\left(\frac{20075\zeta_6}{64}+\frac{663\zeta_4}{4}+\frac{-658048{\zeta_3}^2+482720\zeta_3-3539776\zeta_5-1838592\zeta_7+720901}{4096}\right)Ny^6 \qquad (14)
\end{aligned}
$$

where ζ_n is the Riemann zeta-function. Equally for β_y we find

$$
\begin{aligned}
\beta_y^{(1)} &= 2Ny^2+3y^2\\
\beta_y^{(2)} &= 24\lambda^2y-24\lambda y^2-6Ny^3-\frac{9y^3}{8}\\
\beta_y^{(3)} &= -216\lambda^3y-90\lambda^2Ny^2+273\lambda^2y^2+90\lambda Ny^3+126\lambda y^3+\frac{7N^2y^4}{2}+\frac{1}{32}\left(432\zeta_3+67\right)Ny^4+\frac{1}{64}\left(912\zeta_3-697\right)y^4\\
\beta_y^{(4)} &= 14040\lambda^4y+288\lambda^3Ny^2+36\left(144\zeta_3-455\right)\lambda^3y^2-12\lambda^2N^2y^3+2\left(324\zeta_3-635\right)\lambda^2Ny^3-\frac{135}{2}\left(40\zeta_3+33\right)\lambda^2y^3\\
&\quad+12\lambda N^2y^4-\left(648\zeta_3+683\right)\lambda Ny^4-\frac{3}{8}\left(1008\zeta_3+943\right)\lambda y^4+\frac{11N^3y^5}{6}+\left(\frac{27}{2}\zeta_4-\frac{125\zeta_3}{2}-\frac{899}{24}\right)N^2y^5\\
&\quad+\left(\frac{69}{2}\zeta_4-\frac{331\zeta_3}{2}-105\zeta_5+\frac{9907}{64}\right)Ny^5+\left(\frac{171}{8}\zeta_4+\frac{5\zeta_3}{8}-\frac{215\zeta_5}{2}+\frac{30529}{512}\right)y^5\\
\beta_y^{(5)} &= -\frac{216}{5}\left(5760\zeta_4-2160\zeta_3+18545\right)\lambda^5y-126\left(72\zeta_3+479\right)\lambda^4Ny^2\\
&\quad+12\left(19116\zeta_4-16038\zeta_3-34560\zeta_5+77665\right)\lambda^4y^2+162\left(8\zeta_3+9\right)\lambda^3N^2y^3\\
&\quad+\left(8748\zeta_4-55620\zeta_3+84621\right)\lambda^3Ny^3+\left(-36450\zeta_4+33822\zeta_3+198720\zeta_5+\frac{980055}{8}\right)\lambda^3y^3\\
&\quad+\frac{21}{2}\left(24\zeta_3+5\right)\lambda^2N^3y^4+\left(1215\zeta_4-3573\zeta_3-\frac{3399}{2}\right)\lambda^2N^2y^4\\
&\quad+\left(-4509\zeta_4+\frac{96537\zeta_3}{2}-15360\zeta_5+\frac{463091}{16}\right)\lambda^2Ny^4+\left(-\frac{15255\zeta_4}{4}+29601\zeta_3+22725\zeta_5+\frac{291657}{32}\right)\lambda^2y^4\\
&\quad-\frac{21}{2}\left(24\zeta_3+5\right)\lambda N^3y^5+\left(-1215\zeta_4+3411\zeta_3+3115\right)\lambda N^2y^5\\
&\quad+\left(-\frac{2007\zeta_4}{2}+\frac{16629\zeta_3}{2}+11100\zeta_5-\frac{110555}{32}\right)\lambda Ny^5-\frac{3}{64}\left(12720\zeta_4-80768\zeta_3-53280\zeta_5+5603\right)\lambda y^5\\
&\quad+\left(\frac{19}{16}-3\zeta_3\right)N^4y^6+\left(-\frac{1125\zeta_4}{16}+\frac{2707\zeta_3}{16}+26\zeta_5+\frac{3477}{128}\right)N^3y^6\\
&\quad+\left(-\frac{1575\zeta_6}{8}-\frac{6093\zeta_4}{32}+\frac{273{\zeta_3}^2}{4}+\frac{16345\zeta_3}{32}+\frac{5259\zeta_5}{4}-\frac{272751}{512}\right)N^2y^6\\
&\quad+\left(-\frac{3975\zeta_6}{8}-\frac{2439\zeta_4}{8}+\frac{1}{512}\left(175296{\zeta_3}^2-43816\zeta_3+721360\zeta_5+431928\zeta_7-583115\right)\right)Ny^6\\
&\quad+\left(\frac{109305\zeta_7}{128}-\frac{321669}{2048}-\frac{9675\zeta_6}{32}-\frac{2103\zeta_5}{64}-\frac{189\zeta_4}{64}-\frac{61227\zeta_3}{128}+\frac{2241{\zeta_3}^2}{8}\right)y^6\,. \qquad (15)
\end{aligned}
$$

B. Anomalous dimensions

For the field anomalous dimensions we define

$$\gamma_\psi = \sum_{L=1}^{5} \gamma_\psi^{(L)}, \quad \gamma_\phi = \sum_{L=1}^{5} \gamma_\phi^{(L)} \tag{16}$$

with

$$\begin{aligned}
\gamma_\psi^{(1)} &= \frac{y}{2} \\
\gamma_\psi^{(2)} &= -\frac{3Ny^2}{4} - \frac{y^2}{16} \\
\gamma_\psi^{(3)} &= -\frac{33\lambda^2 y}{2} + 6\lambda y^2 - \frac{3}{8}N^2y^3 + \frac{47Ny^3}{32} + \frac{3}{128}\left(16\zeta_3 - 5\right)y^3 \\
\gamma_\psi^{(4)} &= 342\lambda^3 y + 84\lambda^2 Ny^2 + \left(54\zeta_3 - \frac{641}{4}\right)\lambda^2 y^2 - \frac{87}{2}\lambda N y^3 + \frac{3}{8}\left(32\zeta_3 - 93\right)\lambda y^3 + \left(\zeta_3 - \frac{3}{16}\right)N^3y^4 \\
&\quad -\frac{73}{24}N^2y^4 + \left(-\frac{9}{8}\zeta_4 - \frac{107\zeta_3}{16} + \frac{835}{384}\right)Ny^4 + \left(-\frac{15}{16}\zeta_4 - \frac{9\zeta_3}{4} - \frac{5\zeta_5}{4} + \frac{4465}{1024}\right)y^4 \\
\gamma_\psi^{(5)} &= -18\left(54\zeta_3 + 935\right)\lambda^4 y - \frac{1971}{2}\lambda^3 Ny^2 + \left(243\zeta_4 - 5589\zeta_3 + \frac{156147}{16}\right)\lambda^3 y^2 + \left(9\zeta_3 + \frac{123}{8}\right)\lambda^2 N^2 y^3 \\
&\quad + \frac{1}{40}\left(2430\zeta_4 - 43470\zeta_3 + 50245\right)\lambda^2 N y^3 + \left(\frac{3213\zeta_4}{8} + 522\zeta_3 - 810\zeta_5 + \frac{12455}{16}\right)\lambda^2 y^3 + \left(\frac{63}{8} - 9\zeta_3\right)\lambda N^2 y^4 \\
&\quad + \left(63\zeta_4 + \frac{1005\zeta_3}{4} - 105\zeta_5 + \frac{8717}{32}\right)\lambda N y^4 + \frac{3\left(20880\zeta_4 + 95\left(544\zeta_3 - 800\zeta_5 + 393\right)\right)\lambda y^4}{1280} \\
&\quad + \frac{3}{160}\left(80\zeta_4 - 80\zeta_3 - 5\right)N^4y^5 + \frac{1}{40}\left(90\zeta_4 - 50\zeta_3 - 155\right)N^3y^5 + \frac{1}{960}\left(855\zeta_4 + 35805\zeta_3 - 3120\zeta_5 + 7930\right)N^2y^5 \\
&\quad + \left(\frac{425\zeta_6}{32} - \frac{69\zeta_4}{64} - \frac{5{\zeta_3}^2}{16} + \frac{6789\zeta_3}{128} + \frac{117\zeta_5}{4} - \frac{492529}{6144}\right)Ny^5 \\
&\quad + \left(\frac{1323\zeta_7}{256} - \frac{87335}{4096} + \frac{775\zeta_6}{64} + \frac{2927\zeta_5}{128} - \frac{639\zeta_4}{128} - \frac{3225\zeta_3}{256} + \frac{43{\zeta_3}^2}{16}\right)y^5
\end{aligned} \tag{17}$$

and

$$\begin{aligned}
\gamma_\phi^{(1)} &= 2Ny \\
\gamma_\phi^{(2)} &= 24\lambda^2 - \frac{5Ny^2}{2} \\
\gamma_\phi^{(3)} &= -216\lambda^3 - 90\lambda^2 Ny + 30\lambda N y^2 + \frac{25N^2y^3}{4} + \frac{3}{32}\left(16\zeta_3 + 7\right)Ny^3 \\
\gamma_\phi^{(4)} &= 14040\lambda^4 + 288\lambda^3 Ny - 12\lambda^2 N^2y^2 + 8\left(81\zeta_3 - 91\right)\lambda^2 Ny^2 - 76\lambda N^2y^3 + 3\left(16\zeta_3 - 83\right)\lambda N y^3 \\
&\quad + \left(\frac{101}{24} - 6\zeta_3\right)N^3y^4 + \left(-\frac{9}{2}\zeta_4 - \frac{53\zeta_3}{2} + \frac{211}{24}\right)N^2y^4 - \frac{1}{8}\left(30\zeta_4 + 123\zeta_3 + 40\zeta_5 - 145\right)Ny^4 \\
\gamma_\phi^{(5)} &= -216\left(1152\zeta_4 - 432\zeta_3 + 3709\right)\lambda^5 - 126\left(72\zeta_3 + 479\right)\lambda^4 Ny + 162\left(8\zeta_3 + 9\right)\lambda^3 N^2y^2 \\
&\quad -54\left(90\zeta_4 + 598\zeta_3 - 751\right)\lambda^3 Ny^2 + \frac{21}{2}\left(24\zeta_3 + 5\right)\lambda^2 N^3y^3 + \left(1215\zeta_4 - 2979\zeta_3 + \frac{4863}{4}\right)\lambda^2 N^2y^3 \\
&\quad + \left(\frac{6993\zeta_4}{2} - 993\zeta_3 - 5640\zeta_5 + \frac{167039}{16}\right)\lambda^2 Ny^3 - \frac{157}{2}\lambda N^3y^4 + \left(90\zeta_4 + 933\zeta_3 - 420\zeta_5 + \frac{6709}{8}\right)\lambda N^2y^4 \\
&\quad + \left(\frac{1359\zeta_4}{4} + \frac{1263\zeta_3}{2} - \frac{1425\zeta_5}{2} + \frac{43175}{64}\right)\lambda N y^4 + \left(-9\zeta_4 + 4\zeta_3 + \frac{27}{8}\right)N^4y^5 \\
&\quad + \left(-\frac{477\zeta_4}{16} + \frac{1483\zeta_3}{16} + 2\zeta_5 + \frac{21271}{384}\right)N^3y^5 + \left(\frac{425\zeta_6}{8} - \frac{39\zeta_4}{2} + \frac{{\zeta_3}^2}{4} + \frac{1071\zeta_3}{4} + \frac{473\zeta_5}{4} - \frac{520729}{1536}\right)N^2y^5 \\
&\quad + \left(\frac{1323\zeta_7}{64} - \frac{126057}{1024} + \frac{775\zeta_6}{16} + \frac{3777\zeta_5}{32} - \frac{585\zeta_4}{32} - \frac{531\zeta_3}{32} + \frac{37{\zeta_3}^2}{4}\right)Ny^5 \,.
\end{aligned} \tag{18}$$

Finally for the scalar mass operator we have

$$
\begin{aligned}
\gamma_{\phi^2}^{(1)} &= -12\lambda \\
\gamma_{\phi^2}^{(2)} &= 144\lambda^2 + 24\lambda Ny - 2Ny^2 \\
\gamma_{\phi^2}^{(3)} &= -6264\lambda^3 - 288\lambda^2 Ny + 36\lambda N^2y^2 - \frac{3}{2}\left(120\zeta_3 + 11\right)\lambda Ny^2 - 16N^2y^3 - 12\left(\zeta_3 - 3\right)Ny^3 \\
\gamma_{\phi^2}^{(4)} &= 1728\left(36\zeta_4 + 18\zeta_3 + 187\right)\lambda^4 + 36\left(96\zeta_3 + 313\right)\lambda^3 Ny - 96\left(3\zeta_3 + 11\right)\lambda^2 N^2y^2 \\
&\quad + 6\left(216\zeta_4 + 1440\zeta_3 + 949\right)\lambda^2 Ny^2 + \left(48 - 96\zeta_3\right)\lambda N^3y^3 + \left(-360\zeta_4 + 504\zeta_3 + \frac{2427}{2}\right)\lambda N^2y^3 \\
&\quad + \left(-621\zeta_4 + 960\zeta_3 + 1080\zeta_5 - \frac{38967}{16}\right)\lambda Ny^3 + \left(36\zeta_3 - 22\right)N^3y^4 \\
&\quad + \left(27\zeta_4 + 10\zeta_3 + 140\zeta_5 - \frac{651}{4}\right)N^2y^4 + \left(-63\zeta_4 - 84\zeta_3 + \frac{315\zeta_5}{2} - \frac{1423}{32}\right)Ny^4 \\
\gamma_{\phi^2}^{(5)} &= -108\left(86400\zeta_6 + 39744\zeta_4 + \left(-20736{\zeta_3}^2 + 72048\zeta_3 + 2304\zeta_5 + 166267\right)\right)\lambda^5 \\
&\quad - 18\left(13392\zeta_4 + 19392\zeta_3 + 6912\zeta_5 + 23237\right)\lambda^4 Ny + \frac{9}{10}\left(10080\zeta_4 + 6240\zeta_3 + 92365\right)\lambda^3 N^2y^2 \\
&\quad - \frac{3}{4}\left(345600\zeta_6 + 9648\zeta_4 + 82944{\zeta_3}^2 + 606960\zeta_3 + 55296\zeta_5 + 908231\right)\lambda^3 Ny^2 - 144\left(\frac{9\zeta_4}{2} - 27\zeta_3 + 11\right)\lambda^2 N^3y^3 \\
&\quad + \frac{9}{4}\left(3600\zeta_4 - 13216\zeta_3 - 1440\zeta_5 - 37163\right)\lambda^2 N^2y^3 \\
&\quad + \left(51300\zeta_6 + 27594\zeta_4 - 26568{\zeta_3}^2 - 25200\zeta_3 - 70668\zeta_5 + \frac{972023}{8}\right)\lambda^2 Ny^3 \\
&\quad + \left(-180\zeta_4 + 120\zeta_3 + 60\right)\lambda N^4y^4 + \left(378\zeta_4 - 1569\zeta_3 - 540\zeta_5 + \frac{19641}{8}\right)\lambda N^3y^4 \\
&\quad + \left(225\zeta_6 + \frac{10377\zeta_4}{4} - 2718{\zeta_3}^2 - \frac{8763\zeta_3}{4} - 19947\zeta_5 + \frac{1811931}{128}\right)\lambda N^2y^4 \\
&\quad + \left(\frac{23925\zeta_6}{4} + \frac{85545\zeta_4}{16} - \frac{3}{256}\left(221312{\zeta_3}^2 - 121232\zeta_3 + 891904\zeta_5 + 604128\zeta_7 - 867809\right)\right)\lambda Ny^4 \\
&\quad + 4\left(18\zeta_4 - 10\zeta_3 - 7\right)N^4y^5 + \left(350\zeta_6 + 96\zeta_4 + 68{\zeta_3}^2 - 66\zeta_3 - 714\zeta_5 - \frac{57691}{96}\right)N^3y^5 \\
&\quad + \left(\frac{4725\zeta_6}{4} - \frac{1701\zeta_4}{4} - \frac{3{\zeta_3}^2}{2} + \frac{1129\zeta_3}{4} - \frac{1847\zeta_5}{2} - 1603\zeta_7 + \frac{1274651}{768}\right)N^2y^5 \\
&\quad + \left(\frac{14325\zeta_6}{16} - \frac{141\zeta_4}{16} + \frac{729{\zeta_3}^2}{8} + \frac{4331\zeta_3}{4} - \frac{7}{512}\left(3680\zeta_5 + 125840\zeta_7 + 25931\right)\right)Ny^5
\end{aligned}
\tag{19}
$$

where

$$
\gamma_{\phi^2} = \sum_{L=1}^{5} \gamma_{\phi^2}^{(L)} \; . \tag{20}
$$

With such a colossal computation it is important to outline the independent checks we carried out to ensure the veracity of the five loop contributions.

First the non-simple poles in ϵ of all the new five loop renormalizations constants pass the check that they are all pre-determined by the simple poles of the lower loop companions due to the basic property of the renormalization group equation.

A second check is established on the computation algorithm at five loops by realizing that setting $y = 0$ in (1) produces a Lagrangian with N free fermions and scalar ϕ^4 theory. Therefore taking the same limit in the renormalization group functions the expressions for γ_ϕ, γ_{ϕ^2} and β_λ should be equivalent to the direct evaluation of these renormalization group functions to five loops given in, for example, [5, 75, 76]. It is reassuring to note that this check is also satisfied after observing that λ has to be rescaled by a factor that ensures the same normalization of the quartic interaction is used in the comparison.

The final check we have undertaken is to compare the critical exponents derived from the renormalization group functions at the Wilson-Fisher fixed point with the same quantities but evaluated in the large N expansion. The latter exponents are available to several orders in powers of $1/N$ with the relevant ones for this check computed in [31, 33–36, 77, 78]. At criticality the exponents depend on two variables which are ϵ and N. Carrying out a double Taylor expansion of the large N exponents in powers of ϵ and $1/N$ produces expressions which overlap with $\mathcal{O}(\epsilon^5)$ perturbatively determined exponents when these are equally expanded in large N. Moreover this check provides a test of the five loop results for non-zero y. In summarizing this procedure we note that fuller details are provided for completeness in Appendix A and record that full consistency was satisfyingly found.

IV. CRITICAL EXPONENTS FOR $N = 2$

Having constructed the full renormalization group equations for the GNY model the next step is to derive the core critical exponents at the Wilson-Fisher fixed point in $d = 4 - \epsilon$ dimensions. Therefore we have first solved (13) for the critical couplings $y^\star$ and $\lambda^\star$ as power series in ϵ to $\mathcal{O}(\epsilon^5)$. These values are then substituted into $\gamma_\psi(\lambda, y)$, $\gamma_\phi(\lambda, y)$ and $\gamma_{\phi^2}(\lambda, y)$ to determine the respective ϵ expansions of $\eta_\psi(\epsilon)$, $\eta_\phi(\epsilon)$ and $\eta_{\phi^2}(\epsilon)$. We have carried this out for a general value of N. As y and λ appear in $\beta_y^{(1)}$ and $\beta_\lambda^{(1)}$ in a coupled way the critical couplings will involve the quantity $\sqrt{(4N^2 + 132N + 9)}$, [17], which evaluates to 17 when $N = 2$ but leads to cumbersome expressions for arbitrary N aside, for example, for $N = 3$ and 9 when integer values also occur. Therefore we have provided them and results in [79]. However as one of our main interests is the case of $N = 2$ we will record the exponents for this value partly for our subsequent analysis but also because the N dependent square root then reduces to an integer. For the two fields their anomalous dimensions are

$$\begin{aligned}\eta_\psi = \frac{1}{14}\epsilon - \frac{71}{10584}\epsilon^2 + \Big(- \frac{2432695}{158696496} - \frac{18}{2401}\zeta_3 \Big)\epsilon^3 + \Big(\frac{150}{16807}\zeta_5 - \frac{27}{4802}\zeta_4 + \frac{11109323}{555437736}\zeta_3 - \frac{111266497289}{11557548410688} \Big)\epsilon^4 \\ + \Big(- \frac{89279362217932877}{11783983899150199296} - \frac{1905116200933}{377546581415808}\zeta_3 - \frac{136650473}{2744515872}\zeta_5 - \frac{5643}{537824}\zeta_7 - \frac{2004}{823543}\zeta_3^2 \\ + \frac{375}{33614}\zeta_6 + \frac{11109323}{740583648}\zeta_4 \Big)\epsilon^5 \; + \; \mathcal{O}(\epsilon^6)\end{aligned} \tag{21}$$

and

$$\begin{aligned}\eta_\phi = \frac{4}{7}\epsilon + \frac{109}{882}\epsilon^2 + \Big(\frac{1170245}{26449416} - \frac{144}{2401}\zeta_3 \Big)\epsilon^3 + \Big(\frac{20491307339}{481564517112} - \frac{108}{2401}\zeta_4 + \frac{1200}{16807}\zeta_5 + \frac{1563532}{23143239}\zeta_3 \Big)\epsilon^4 \\ + \Big(\frac{32079891787774525}{981998658262516608} - \frac{1237285035017}{31462215117984}\zeta_3 - \frac{69575957}{228709656}\zeta_5 - \frac{15885}{823543}\zeta_3^2 - \frac{5643}{67228}\zeta_7 \\ + \frac{1500}{16807}\zeta_6 + \frac{390883}{7714413}\zeta_4 \Big)\epsilon^5 \; + \; \mathcal{O}(\epsilon^6) \; .\end{aligned} \tag{22}$$

Equally the scalar field mass operator exponent is

$$\begin{aligned}\eta_{\phi^2} = \; - \frac{8}{21}\epsilon + \frac{2942}{22491}\epsilon^2 + \Big(\frac{88644929}{2547960408} - \frac{144404}{1102059}\zeta_3 \Big)\epsilon^3 \\ + \Big(\frac{18303692723219}{835032872672208} - \frac{36101}{367353}\zeta_4 + \frac{155735}{1361367}\zeta_5 + \frac{1707335624}{20065188213}\zeta_3 \Big)\epsilon^4 \\ + \Big(\frac{3531904209162553649}{212848209178400474784} - \frac{6505866583}{16524272646}\zeta_5 + \frac{24305439575}{327731407479}\zeta_3^2 + \frac{44217078119105}{6819435126823032}\zeta_3 \\ + \frac{778675}{5445468}\zeta_6 + \frac{8001521}{13714512}\zeta_7 + \frac{426833906}{6688396071}\zeta_4 \Big)\epsilon^5 \; + \; \mathcal{O}(\epsilon^6).\end{aligned} \tag{23}$$

While η_{ϕ^2} is an exponent that is not ordinarily determined experimentally, it is required as an intermediate step to the one that is measured which is $1/\nu$ and derived from the scaling law

$$\frac{1}{\nu} \; = \; 2 \; - \; \eta_\phi \; + \; \eta_{\phi^2} \; . \tag{24}$$

Therefore we have

$$\begin{aligned}\frac{1}{\nu} &= 2 - \frac{20}{21}\epsilon + \frac{325}{44982}\epsilon^2 + \left(- \frac{36133009}{3821940612} - \frac{78308}{1102059}\zeta_3 \right)\epsilon^3 \\ &+ \left(\frac{58535}{1361367}\zeta_5 - \frac{19577}{367353}\zeta_4 + \frac{351753380}{20065188213}\zeta_3 - \frac{17228234202607}{835032872672208} \right)\epsilon^4 \\ &+ \left(- \frac{13685649343350298579}{851392836713601899136} - \frac{5916014759}{66097090584}\zeta_5 + \frac{30626922980}{327731407479}\zeta_3^2 + \frac{1249594437836159}{27277740507292128}\zeta_3 \right. \\ &\left. + \frac{292675}{5445468}\zeta_6 + \frac{9152693}{13714512}\zeta_7 + \frac{87938345}{6688396071}\zeta_4 \right)\epsilon^5 + \mathcal{O}(\epsilon^6)\end{aligned} \tag{25}$$

which completes the set of core exponents that are required for our three dimensional analysis.

In addition we have determined the $\mathcal{O}(\epsilon^5)$ correction to scaling exponents which are denoted by $\omega_\pm$ and are required as part of our check with the large N exponents. They are calculated from the gradients of the β-functions at criticality. In particular these are encoded in a 2×2 matrix

$$\beta_{ij} = \begin{pmatrix} \frac{\partial \beta_y}{\partial y} & \frac{\partial \beta_y}{\partial \lambda} \\ \frac{\partial \beta_\lambda}{\partial y} & \frac{\partial \beta_\lambda}{\partial \lambda} \end{pmatrix} \equiv \begin{pmatrix} \beta_{11} & \beta_{12} \\ \beta_{21} & \beta_{22} \end{pmatrix} \tag{26}$$

which is then evaluated at $y^\star$ and $\lambda^\star$. The final stage is to construct the ϵ expansion of the two perturbative eigenvalues of β_{ij} which correspond to $\omega_\pm$. In order to make a point of connection of our perturbative expressions for $\omega_\pm$ with the earlier large N conventions of [78] we are required to take

$$\omega_\pm = \frac{1}{2}\left(\beta_{11} + \beta_{22}\right) \mp \frac{1}{2}\sqrt{[(\beta_{11} - \beta_{22})^2 + 4\beta_{12}\beta_{21}]} \tag{27}$$

as the appropriate definitions. This leads to the two critical exponents

$$\begin{aligned}\omega_+ &= \frac{17}{7}\epsilon - \frac{47725}{22491}\epsilon^2 + \left(+ \frac{25651541920}{8599366377} + \frac{1219592}{367353}\zeta_3 \right)\epsilon^3 \\ &+ \left(- \frac{45263181593447273}{7515295854049872} - \frac{22241763116}{2866455459}\zeta_3 - \frac{2298610}{151263}\zeta_5 + \frac{304898}{122451}\zeta_4 \right)\epsilon^4 \\ &+ \left(- \frac{5560440779}{955485153}\zeta_4 + \frac{186794373160}{36414600831}\zeta_3^2 + \frac{4733999225077}{99145635876}\zeta_5 + \frac{253430775397933345}{13638870253646064}\zeta_3 \right. \\ &\left. + \frac{6219840998765669078468 87}{45975213182534502553344} - \frac{5746525}{302526}\zeta_6 + \frac{1467290683}{20571768}\zeta_7 \right)\epsilon^5 + \mathcal{O}(\epsilon^6)\end{aligned} \tag{28}$$

and

$$\begin{aligned}\omega_- &= \epsilon - \frac{533}{1512}\epsilon^2 + \left(\frac{165\zeta_3}{686} + \frac{6685099}{34006392} \right)\epsilon^3 \\ &+ \left(\frac{495\zeta_4}{2744} - \frac{61742201\zeta_3}{79348248} - \frac{1905\zeta_5}{4802} - \frac{11065294400875}{59438820397824} \right)\epsilon^4 \\ &+ \left(- \frac{9525\zeta_6}{19208} - \frac{61742201\zeta_4}{105797664} + \frac{195609{\zeta_3}^2}{941192} + \frac{60312023254291\zeta_3}{53935225916544} + \frac{473424095\zeta_5}{196036848} + \frac{46467\zeta_7}{76832} \right. \\ &\left. + \frac{10290966679190176397}{45452509325293625856} \right)\epsilon^5 + \mathcal{O}(\epsilon^6) \, .\end{aligned} \tag{29}$$

The mismatch in the respective leading order coefficients in (29) is due to the ϵ term of ω_- being N independent unlike that of ω_+. In relation to previous work we note that ω_- was denoted by ω in [39] whereas ω_+ corresponds to ω' of the same article. Indeed it was noted in [39] that the large N expansion of the former perturbative eigen-exponent agreed with the ϵ dependence of the $\mathcal{O}(1/N)$ exponent directly determined in [77]. The large N expressions for $\omega_\pm$ at $\mathcal{O}(1/N^2)$ appeared subsequently in [78].

V. ANALYSIS

Having constructed the five loop renormalization group functions our aim in this section is to produce refined estimates for critical exponents in three dimensions for several values of N that correspond to phase transitions in a

variety of physical applications. For instance the critical exponents for $N = 2$ relate to the semi-metal CDW (charge density wave) phase transition of electrons in graphene [15] while the same transition for the spinless fermions on a honeycomb lattice is described by the $N = 1$ GNY universality class. While both these cases are of physical interest we will also analyse $N = 5$ since there are conformal bootstrap estimates available in [28]. We use this as a guidepost on the reliability of the resummation techniques we employ. Although the GN and GNY Lagrangians are renormalizable in two and four dimensions respectively since the models of physical interest are in three dimensions we have to translate the five loop $4 - \epsilon$ exponents to three dimensions. Naively setting $\epsilon = 1$ is problematic on several grounds. For instance when $N = 2$ the numerical evaluation of the exponents gives

$$\begin{aligned}
\eta_\psi &= 0.071429\epsilon - 0.006708\epsilon^2 - 0.024341\epsilon^3 + 0.017584\epsilon^4 - 0.051782\epsilon^5 + \mathcal{O}(\epsilon^6) \\
\eta_\phi &= 0.571429\epsilon + 0.123583\epsilon^2 - 0.027849\epsilon^3 + 0.149112\epsilon^4 - 0.296922\epsilon^5 + \mathcal{O}(\epsilon^6) \\
\frac{1}{\nu} &= 2 - 0.952381\epsilon + 0.007225\epsilon^2 - 0.094868\epsilon^3 - 0.012653\epsilon^4 + 0.823067\epsilon^5 + \mathcal{O}(\epsilon^6)
\end{aligned} \tag{30}$$

where it is evident that the $\mathcal{O}(\epsilon^5)$ terms are the same order of magnitude as the $\mathcal{O}(\epsilon)$ coefficients, unlike the intervening ones, meaning that the series convergence for $\epsilon = 1$ could be questionable. To gauge the situation we have constructed a set of estimates using $[m/n]$ Padé approximants which are recorded in Table I for $N = 2$. Padé estimates were not possible for all choices at four loops. Cases where the approximant was not continuous from four dimensions to below three dimensions due, for instance, to poles in the range were excluded. The two continuous Padé estimates at four loops are in reasonable accord. At five loops the [1/4] values for η_ψ, η_ϕ and ω_- are significantly distant from the other three approximants which is probably related to the fact that they each begin with ϵ. For both η_ϕ and ω_- the other five loop estimates are commensurate with the four loop ones. We note that a Monte Carlo estimate for ω_- of 0.8(1) was provided in [22]. For $1/\nu$ there is more than a 10% difference from the lowest to the highest value which could be a reflection that the five loop term of $1/\nu$ is around the same size as that at one loop with the intermediate values an order of magnitude or more smaller. For η_ψ there appears to be a divergence of values for the three main approximants meaning that there is no real consensus for an estimate at five loops using this canonical Padé analysis.

$N = 2$	η_ψ	η_ϕ	$1/\nu$	ω_-
[2/2]	0.0539	0.7079	0.931	0.794
[3/1]	0.0506	0.6906	0.945	0.777
[1/4]	0.03457	0.4642	1.067	− 1.242
[2/3]	0.05065	0.7251	0.91917	0.7876
[3/2]	0.02044	0.7291	1.039	0.7870
[4/1]	0.04484	0.7170	0.9598	0.7882

TABLE I. L loop $[m/n]$ Padé critical exponent estimates in $d = 3$ where $L = m + n$.

In order to gauge where these naive Padé and later estimates sit from an overall point of view we have provided a compendium of results from other methods in Table II. The entries are listed in chronological order beginning with large N estimates where three terms of each exponent are known in d-dimensions in a $1/N$ expansion. By this we mean η_ϕ and $1/\nu$ have been computed to $\mathcal{O}(1/N^2)$ as each canonical term is non-zero and η_ψ is available at $\mathcal{O}(1/N^3)$ since there is no $\mathcal{O}(1)$ term. The large N estimates should be regarded as being within the same general framework as perturbation theory which includes the three sets of four loop estimates from [40]. For η_ψ there appears to be consistent agreement with results from more recent methods such as the conformal bootstrap results of [29] and [30] which represent the highest precision to date with that method. The four loop naive two dimensional Padé estimates in Table II are the analogues of (30) and the estimates of Table I with the explicit numerical two dimensional ϵ expansions given in (B2). The [4/1] Padé estimate of Table I is compatible with the four loop η_ψ values of Table II. The various perturbative estimates for η_ϕ in Table II are not far out of line with [29] although the four loop approximants of Table II are around 2% lower. For the $1/\nu$ Padé estimates the picture is not as concrete in relation to Table II. Given the degree of consistent estimates of the four loop two-sided Padé and interpolating polynomial estimates with the most recent conformal bootstrap values of [29] it would seem appropriate to extend that analysis with the new four dimensional four loop data.

The basic idea behind the two-sided Padé and interpolating polynomial methods is that of ultraviolet completion. As the spacetime dimension of interest lies between two theories of the same universality class which are the two dimensional GN and the four dimensional GNY models one can construct a function of d such that the ϵ expansion of the function near two and four dimensions equate to the ϵ expansion of one of the exponents η_ψ, η_ϕ and $1/\nu$. Once constructed the function of d is evaluated for $d = 3$. First we focus on the two-sided Padé estimate which was used in

Method and source	η_ψ	η_ϕ	$1/\nu$
Large N [17, 31–36]	0.044	0.743	0.952
Monte Carlo [17]	——	0.754(8)	1.00(4)
Monte Carlo [18]	0.38(1)	0.62(1)	1.20(1)
Functional renormalization group [25]	0.032	0.760	0.982
Functional renormalization group [25]	0.033	0.767	0.978
Functional renormalization group [25]	0.032	0.756	0.982
Functional renormalization group [26]	0.0276	0.7765	0.994(2)
Four loop $d = 2$ naive Padé [37]	0.082	0.745	0.931
Three loop $d = 4$ naive Padé [38]	0.0740	0.672	1.048
Conformal bootstrap [28]	0.044	0.742	0.880
Monte Carlo [20]	——	0.65(3)	1.2(1)
Monte Carlo [21]	——	0.54(6)	1.14(2)
Four loop $d = 4$ naive Padé [39]	0.0539	0.7079	0.931
Four loop $d = 4$ naive Padé [39]	0.0506	0.6906	0.945
Four loop two-sided Padé [40]	0.042	0.735	1.004
Four loop interpolating polynomial [40]	0.043	0.731	0.982
Four loop Padé-Borel [40]	0.043(12)	0.704(15)	0.993(27)
Monte Carlo [22]	0.05(2)	0.59(2)	1.0(1)
Conformal bootstrap [29]	0.04238(11)	0.7329(27)	0.998(12)
Monte Carlo [24]	0.043(12)	0.72(6)	1.07(12)
Conformal bootstrap [30]	——	0.7339(26)	0.998(12)
Functional renormalization group [27]	0.032	0.760	0.982

TABLE II. Summary of previous exponent estimates for $N = 2$.

[40] for instance. Its general definition is

$$\mathcal{P}_{[m/n]}(d) \;=\; \frac{\sum_{p=0}^{m} a_p d^p}{1 + \sum_{q=1}^{n} b_q d^q} \tag{31}$$

where the choice of unity for the denominator polynomial corresponds to a normalization. This means that like the canonical Padé approximant the number of possible estimates increases with loop order. What is different here is that there are more available data to determine the parameters $\{a_p\}$ and $\{b_q\}$. In particular taking a generic d-dimensional exponent $\eta(d)$ its ϵ expansions around the respective critical dimensions are

$$\eta(2+\epsilon) \;=\; \sum_{n=0}^{\infty} \eta_n^{(2)} \epsilon^n \quad , \quad \eta(4-\epsilon) \;=\; \sum_{n=0}^{\infty} \eta_n^{(4)} \epsilon^n \; . \tag{32}$$

where for instance $\eta_0^{(2)}$ and $\eta_1^{(2)}$ are both zero for η_ψ. So amalgamating the known four loop GN model exponents with the five loop GNY ones means that 11 parameters are available to find the $\{a_p\}$ and $\{b_q\}$ values. More generally if the exponent series for each critical dimension are known to L loops then $2(L+1)$ coefficients are available leading in principle to $2(L+1)$ possible approximants which are $\mathcal{P}_{[m/2L+1-m]}(d)$ where $0 \leq m \leq 2L+1$. Like [40] we will follow the convention that only the diagonal approximants, $\mathcal{P}_{[L/L+1]}(d)$ and $\mathcal{P}_{[L+1/L]}(d)$, are reliable and construct estimates for those. As noted in [40] continuity of each $\mathcal{P}_{[m/n]}(d)$ in $2 \leq d \leq 4$ is not guaranteed.

The second technique we will examine is that of using an interpolating polynomial [40]. Instead of constructing a d-dependent rational polynomial a canonical polynomial is constructed where the coefficients are fixed from both ϵ expansions of a critical exponent. More particularly the polynomial is expressed in powers of $(d-2)$ so that the coefficients of the initial terms of the polynomial are given by those of the GN model. Then the higher order coefficients are determined from the ϵ expansion of the GNY theory in $d = 4 - \epsilon$ dimensions. Specifically

$$\mathcal{I}_{[i,j]}(d) \;=\; \sum_{m=0}^{i} \eta_m^{(2)} (d-2)^m \;+\; \sum_{n=i+1}^{i+j+1} c_n (d-2)^n \tag{33}$$

Padé	η_ψ	η_ϕ	$1/\nu$
[1/2]	——	0.786885	1.012048
[2/1]	——	0.812500	1.000000
[2/3]	——	0.756156	——
[3/2]	0.045930	0.752752	——
[3/4]	0.038789	0.701041	——
[4/3]	0.040184	0.727706	——
[4/5]	0.043732	0.734702	0.978327
[5/4]	0.041742	0.734696	1.004079
[5/5]	0.041418	0.734530	1.021288

TABLE III. Two-sided Padé exponent estimates $\mathcal{P}_{[m/n]}(3)$ for $N = 2$.

Polynomial	η_ψ	η_ϕ	$1/\nu$
[1, 1]	0.017857	0.809524	1.011905
[1, 2]	0.034037	0.774943	1.025616
[2, 2]	0.033636	0.753047	0.994951
[2, 3]	0.036652	0.746200	1.003792
[3, 3]	0.038991	0.731170	0.976204
[3, 4]	0.040071	0.739556	0.987315
[4, 4]	0.042592	0.731413	0.981959
[4, 5]	0.041117	0.730924	1.010424

TABLE IV. Interpolating polynomial $\mathcal{I}_{[i,j]}(3)$ exponent estimates for $N = 2$.

defines the interpolating polynomial [40] where the $\{c_n\}$ are deduced from the condition that expanding around $d = 4 - \epsilon$ reproduces the known coefficient of the same exponent. It is worth noting that if instead $\mathcal{I}_{[i,j]}(d)$ was defined as a series in $(d-4)$ then the *same* polynomial in d would ultimately be produced. One advantage of using $\mathcal{I}_{[i,j]}(d)$ is that the function is continuous and cannot be singular unlike $\mathcal{P}_{[i/j]}(d)$. While this means a large number of estimates can be produced for each exponent from the ranges $1 \leq i \leq 4$ and $1 \leq j \leq 5$ we will focus on the estimates $\mathcal{I}_{[L,L]}(d)$ and $\mathcal{I}_{[L,L+1]}(d)$ at L loops. The former is the natural choice as loop order increases but we include the latter in the analysis in order to see if any pattern is present when there is a mismatch in the number of terms available in the ϵ expansion in the respective critical dimensions. For both polynomial constructions we have solved for the respective unknown parameters in terms of the generic known coefficients of the respective series of (32). This allowed us to construct procedures, as functions of the generic coefficients $\eta_n^{(2)}$ and $\eta_n^{(4)}$, in the computer algebra package `Reduce`. Consequently evaluating the procedures with the explicit coefficients for a particular value of N allows us to quickly determine estimates. We chose not to construct explicit N-dependent expressions as they would be singular at $N = \frac{1}{2}$.

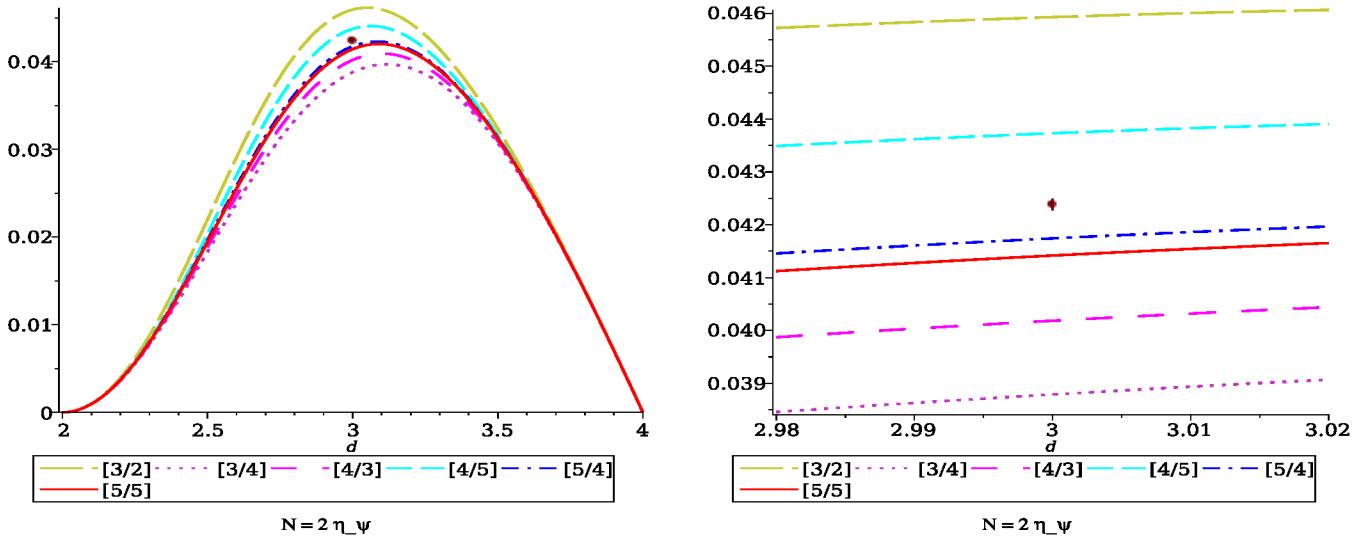

FIG. 2. Two-sided Padé approximants for η_ψ with $N = 2$ in $2 \leq d \leq 4$ (left panel) and $2.98 \leq d \leq 3.02$ (right panel)

A. Graphene case $N = 2$

Having summarized the two techniques employed to obtain exponent estimates we now focus on three particular cases. The first concerns the CDW transition in graphene [15] corresponding to the value of $N = 2$. Estimates for the two-sided Padé and interpolating polynomial are presented in Tables III and IV respectively. The two-sided Padé approximants for η_ϕ were free from poles while those for η_ψ were continuous for both approximations from three loops. For $1/\nu$ reliable estimates did not appear until four and five loops. In this case comparing with latest conformal

bootstrap estimates recorded in the last two lines of Table II the [5/5] value lies two σ from the central value whereas that for [5/4] is within one σ. Including two dimensional five loop information for [5/6] and [6, 5] may mean they are accommodated within the bootstrap uncertainty. This is partly confirmed from the behaviour of η_ϕ as its estimates clearly progress with loop order to values within both bootstrap uncertainties. For η_ψ its progression is not as settled in comparison with the bootstrap. However we note that as the ultimate value is generally accepted as small this means it is difficult to precisely measure which is partially reflected in the range of values in Table II. For the interpolating polynomial estimates of Table IV we recall the L loop estimates correspond to $\mathcal{I}_{[L,L]}$. While the four loops values were computed in [40] these were prior to [29, 30]. So it is worth commenting on the estimates in relation to that more recent work. For both $1/\nu$ and η_ϕ their [4, 4] values are on the edge of both bootstrap uncertainties. Interestingly that for η_ψ is also on the periphery of the estimate of [29]. We included $\mathcal{I}_{[L,L+1]}(3)$ estimates for each loop to gauge the effect of adding in five loop information. For [4, 5] $1/\nu$ is on the upper edge of the bootstrap uncertainty whereas η_ϕ is within that of [29]. For η_ψ the situation is not as clear being 3% different from the bootstrap value in contrast to the 0.5% difference of the [4, 4] value.

While the tables indicate the numerical estimates with the increase of loop order it is more instructive to appreciate the consequences graphically. Therefore we have provided a set of plots for the two-sided Padé approximants in Figures 2, 3 and 4 with the analogous plots for the interpolating polynomial approach given in Figures 5, 6 and 7. In each figure the plot on the left side represents the d-dimensional estimate of the exponent in the full range $2 \leq d \leq 4$ whereas on each right hand side we focus on the same plot but where d lies between 2.98 and 3.02. This is because for η_ϕ and $1/\nu$ the lines are virtually indistinguishable in the full range. In addition we include a point in three dimensions which is the conformal bootstrap estimate of [29]. The error bars are included for each of these points. However in the case of η_ψ they are relatively small compared to the actual point in the plots even in those focussed on the neighbourhood of three dimensions. For plots of the Padé approximants we included those for [3/2] and higher loops for η_ψ and η_ϕ but illustrated all five continuous and pole free ones for $1/\nu$. In the interpolating polynomial plots we present the behaviour of $\mathcal{I}_{[L,L]}(d)$ as well as $\mathcal{I}_{[4,5]}(d)$. In all of the plots the solid line corresponds to the case where five loop information has been included.

In general terms from the structure of the d-dimensional behaviour of the exponents using both techniques it is clear that as loop order increases there is at least qualitative convergence to expected properties. For instance ψ is a free field in both the GN model and GNY theory meaning that η_ψ in d-dimensions has to have a turning point. In Figure 2 the absence of the low loop approximants should not cloud the comparison with Figure 5 which includes the one and two loop polynomials with these corresponding to the lower two of the five lines. The higher loop plots in that case suggest there is oscillatory convergence towards the conformal bootstrap point which is more apparent in the focussed plot in Figure 5. Moreover there is no symmetry of the shape of the plots around three dimensions for either method as expected. For instance the tangents to η_ψ at two and four dimensions have different slopes. In the neighbourhood of two dimensions η_ψ is quadratic. Near four dimensions the gradient has to be negative for instance since η_ψ extends beyond four dimensions towards the fermionic theory in six dimensions that is the ultraviolet extension of the GNY theory. For the theory in that higher dimension ψ will also be a free field. In principle if the renormalization group functions of its Lagrangian were available then additional information could be included in the

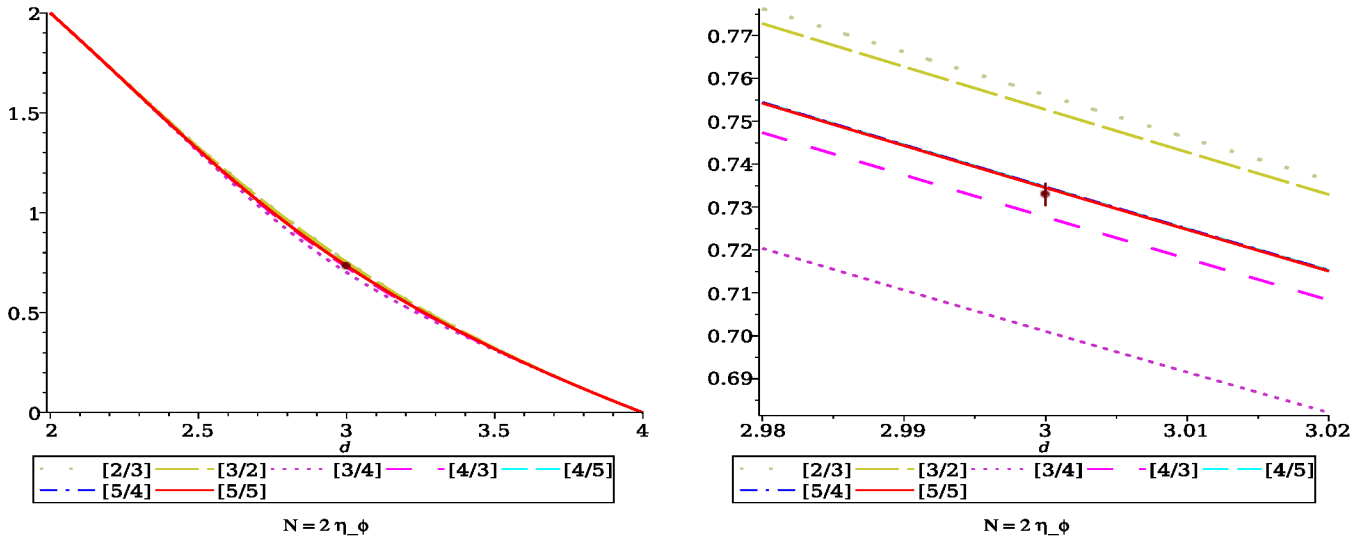

FIG. 3. Two-sided Padé approximants for η_ϕ with $N = 2$ in $2 \leq d \leq 4$ (left panel) and $2.98 \leq d \leq 3.02$ (right panel)

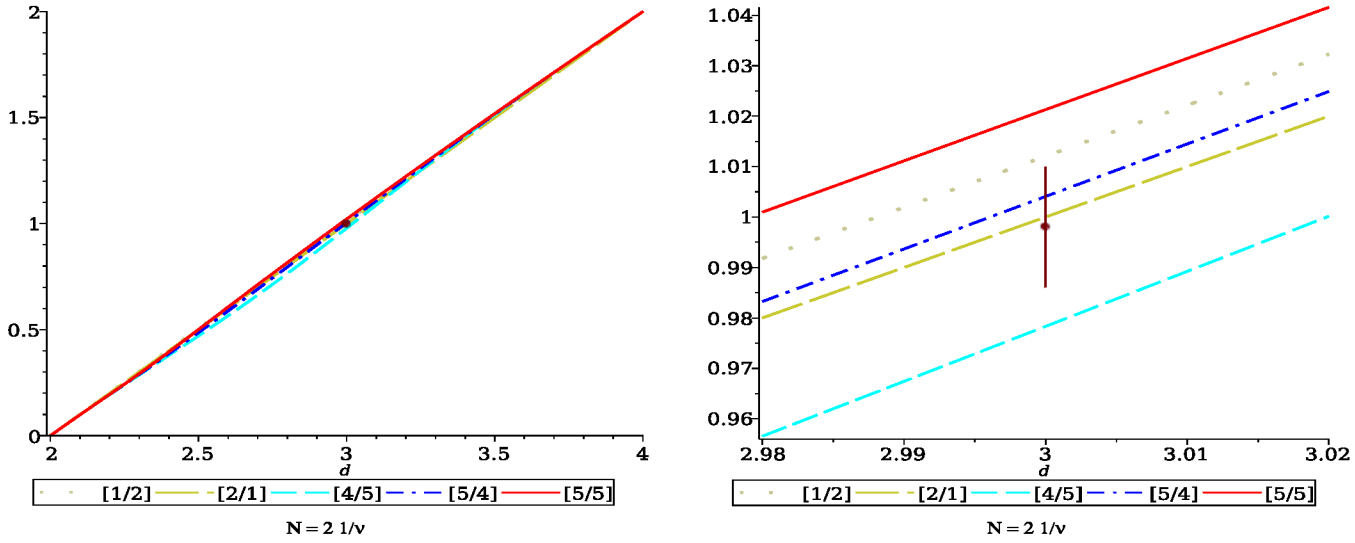

FIG. 4. Two-sided Padé approximants for $1/\nu$ with $N = 2$ in $2 \leq d \leq 4$ (left panel) and $2.98 \leq d \leq 3.02$ (right panel)

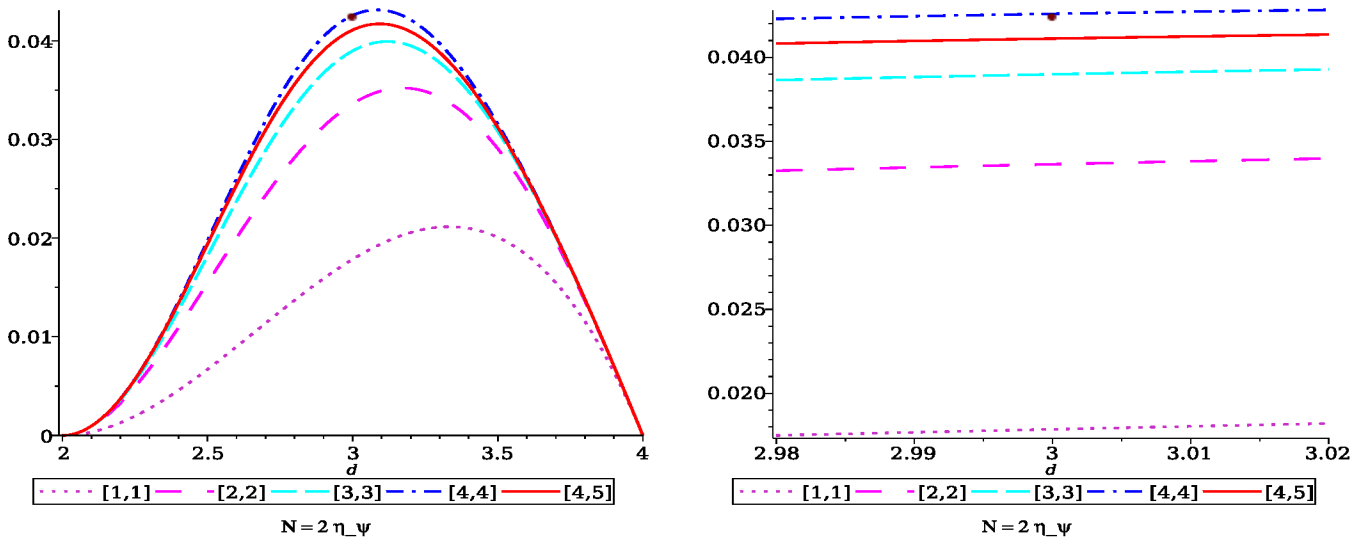

FIG. 5. Interpolating polynomials for η_ψ with $N = 2$ in $2 \leq d \leq 4$ (left panel) and $2.98 \leq d \leq 3.02$ (right panel)

Padé and interpolating polynomial analyses. Although it is not clear if there would be a significant change in our three dimensional estimates. If one considers the gradient of the tangent to η_ψ in the region $3.5 \leq d \leq 3.9$ in Figures 2 and 5 and then extrapolate its trajectory to estimate a value in three dimensions it is evident that it will exceed the exponent estimates. Repeating this exercise for the tangent in the range 2.3 to 2.6 then a similar overestimate will result. This in effect lies behind the overshoot of η_ψ estimates given from the four dimensional one-sided [2/3] Padé value in Table I as well as the two dimensional equivalent in Table II. The latter being larger than the former overshoot is primarily driven by the tangent slopes in the regions either side of three dimensions. The behaviour of η_ϕ and $1/\nu$ differs significantly from η_ψ as both are monotonic functions resulting from their two and four dimensional values being different integers. Indeed the [2/1] Padé approximant for $1/\nu$ is precisely the straight line $d - 2$. The plots of each of these exponents from the two techniques show very similar behaviour in that the small differences in each approximation only become evident in the plots around three dimensions. For η_ϕ the two highest loop order approximations touch the conformal bootstrap error bar and both lines are virtually on top of each other. While it is tempting to claim that there is good convergence that would have to wait until there is a five loop GN analysis. For $1/\nu$ the comparison between both techniques is not as concrete. If one ignores the low loop plots of $\mathcal{P}_{[1/2]}(d)$ and $\mathcal{P}_{[2/1]}(d)$ in Figure 4 then the bootstrap point is bounded by $\mathcal{P}_{[4/5]}(d)$ and $\mathcal{P}_{[5/4]}(d)$. As $\mathcal{P}_{[5/5]}(d)$ lies above $\mathcal{P}_{[5/4]}(d)$ any five loop input from two dimensions to produce $\mathcal{P}_{[5/6]}(d)$ and $\mathcal{P}_{[6/5]}(d)$ would have to lie within the four loop

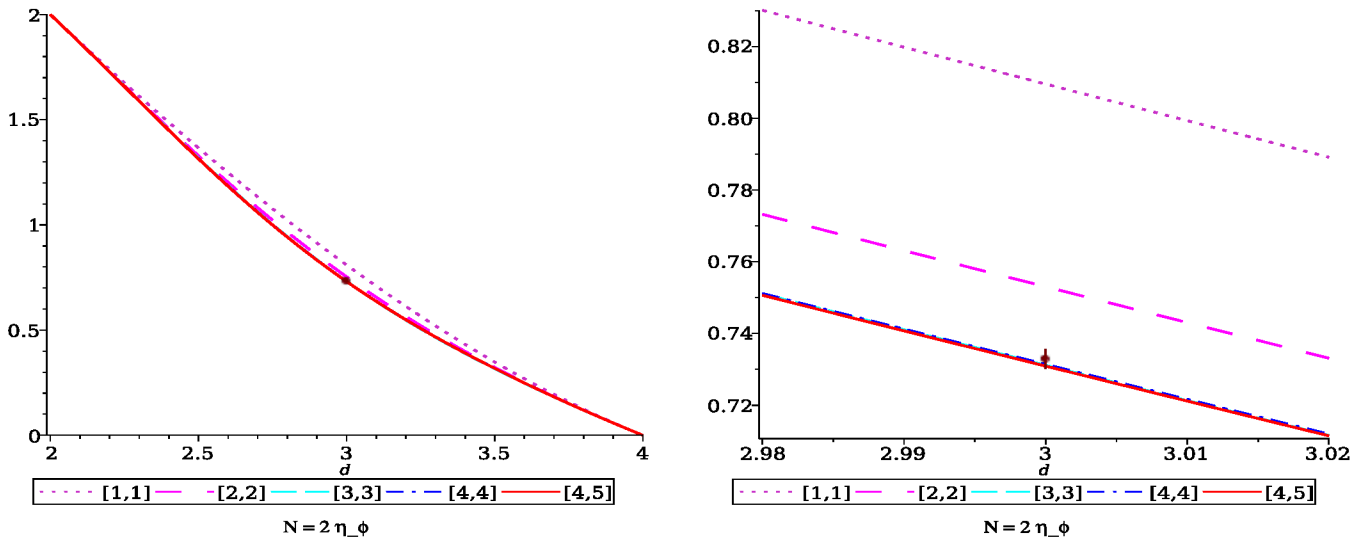

FIG. 6. Interpolating polynomials for η_ϕ with $N = 2$ in $2 \leq d \leq 4$ (left panel) and $2.98 \leq d \leq 3.02$ (right panel)

counterparts to point towards convergence near the value of [29]. By contrast in Figure 7 $\mathcal{I}_{[3,3]}(d)$ and $\mathcal{I}_{[4,4]}(d)$ appear to be creeping towards the lower edge of the conformal bootstrap estimate but the $\mathcal{I}_{[4,5]}(d)$ curve overshoots. Again a better understanding of the trend would require a full five loop comparison.

B. Other cases

Although the $N = 2$ GNY theory has a major physical application several other values of N are of interest and we briefly summarize a similar analysis to that of graphene for $N = 1$ and 5. The former governs semi-metal transitions for spinless fermions on a honeycomb lattice whereas we consider the latter case in order to compare with conformal bootstrap and functional renormalization group results. First for $N = 1$ we provide a summary of exponent estimates from a variety of techniques in Table V. It has parallels to the $N = 2$ summary table in that estimates for η_ψ have a wide range whereas there is mostly a better consensus for η_ϕ and $1/\nu$. Tables VI and VII record our two-sided Padé and interpolating polynomial estimates. The former is more sparse than the graphene case which is due to poles appearing in $2 \leq d \leq 4$ with only one such instance occurring for η_ϕ. The incompleteness of estimates for all three

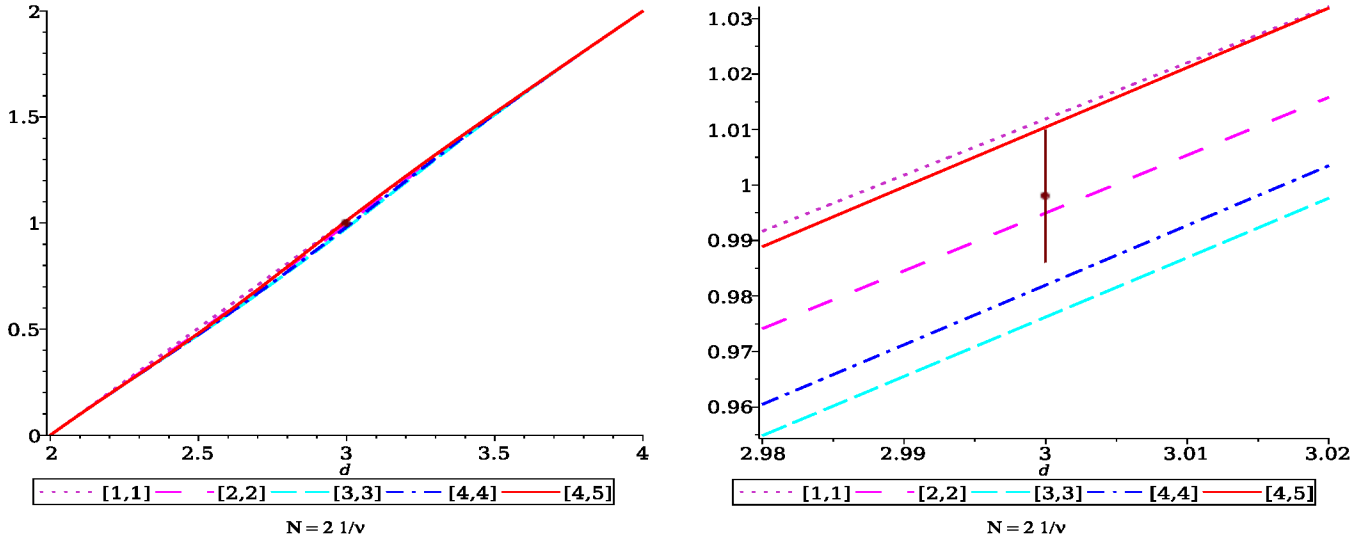

FIG. 7. Interpolating polynomials for $1/\nu$ with $N = 2$ in $2 \leq d \leq 4$ (left panel) and $2.98 \leq d \leq 3.02$ (right panel)

Method and source	η_ψ	η_ϕ	$1/\nu$
Large N [32–36]	0.1056	0.509	0.961
Four loop two-sided Padé [40]	(0.086)	(0.480)	(0.961)
Four loop interpolating polynomial [40]	0.140	0.397	1.040
Four loop Padé-Borel [40]	0.102(12)	0.487(12)	1.114(33)
Monte Carlo [19]	——	0.45(2)	1.30(5)
Functional renormalization group [26]	0.0654	0.5506	1.075(4)
Three loop $d = 4$ naive Padé [38]	0.102	0.463	1.166
Conformal bootstrap [28]	0.084	0.544	0.76
Monte Carlo [21]	——	0.54(6)	1.14(2)
Four loop $d = 4$ naive Padé [39]	0.0976	0.4969	——
Four loop $d = 4$ naive Padé [39]	0.0972	0.4872	——
Four loop $d = 4$ naive Padé [39]	——	——	1.101
Monte Carlo [23]	——	0.51(3)	1.124(13)
Conformal bootstrap [29]	0.08712(32)	0.5155(30)	1.101(10)
Conformal bootstrap [30]	——	0.5156(30)	1.101(10)

TABLE V. Summary of previous exponent estimates for $N = 1$.

exponents prevents any general convergence trends emerging. Instead all we can deduce is that there is a broad general agreement with results provided in Table V. Although the interpolating polynomial method has by construction no continuity problems the $N = 1$ estimates also do not show a convergence path. Only the higher loop estimates for $1/\nu$ are within previous results of Table V. For η_ϕ the $\mathcal{I}_{[i,j]}(3)$ values are unsurprisingly more in line with other perturbative results rather than conformal bootstrap, Monte Carlo and functional renormalization group techniques. It may be the case that several more orders in perturbation theory would be required to obtain commensurate estimates.

Padé	η_ψ	η_ϕ	$1/\nu$
[1/2]	——	0.615385	1.043101
[2/1]	——	0.625000	1.000000
[2/3]	——	0.564955	——
[3/2]	0.107695	0.562831	——
[3/4]	0.074744	0.401109	0.922860
[4/3]	0.090275	0.479073	——
[4/5]	0.098936	0.479788	——
[5/4]	——	——	0.961217
[5/5]	——	0.507009	1.120413

TABLE VI. Two-sided Padé exponent estimates $\mathcal{P}_{[m/n]}(3)$ for $N = 1$.

Polynomial	η_ψ	η_ϕ	$1/\nu$
[1, 1]	0.025000	0.600000	1.041320
[1, 2]	0.052560	0.600613	1.081212
[2, 2]	0.079405	0.419057	0.988436
[2, 3]	0.072515	0.489743	1.042067
[3, 3]	0.116265	0.371511	0.950413
[3, 4]	0.097376	0.450625	1.005131
[4, 4]	0.139895	0.397030	1.039686
[4, 5]	0.111856	0.435192	1.072936

TABLE VII. Interpolating polynomial $\mathcal{I}_{[i,j]}(3)$ exponent estimates for $N = 1$.

Turning to the case of $N = 5$ there has not been the same volume of activity to extract critical exponents both analytically and numerically. This is reflected in the summary of the current situation in Table VIII. Unlike the $N = 1$ case there is a greater general consensus as to the rough values of the three exponents. However all estimates employ continuum field theory approaches as there are no results from lattice field theory or discrete models which would produce Monte Carlo values. The results of our two-sided Padé and interpolating polynomial methods are displayed in Tables IX and X respectively. For the former more approximants are continuous and pole free compared to $N = 1$ with a full set available for η_ϕ. From examining the singular Padé approximants for each of our three values of N it is generally the case that either a simple pole appears in $2 < d < 4$ above two dimensions or there is a pair of poles in the regions either side of three dimensions. Then by looking at the d dependence for the same approximants as N increases the poles above two dimensions move towards the origin or evaporate. Equally where there is a simple pole above three dimensions it translates towards six dimensions. We note that the absence of [3/4] and [5/4] approximants for $1/\nu$ when $N = 5$ is due to the presence of a zero and simple pole which are located within 10^{-4} or less of each other. This was an unusual occurrence across all our Padé analyses. For the interpolating polynomial estimates there were obviously no such hindrances and values listed in Table X show a converging trend for η_ψ and η_ϕ. For $1/\nu$ there

is a similar direction except that the final value increases indicating that a lower dimensional computation would be needed to clarify the situation. Both techniques however show good consistency with the various estimates given in Table VIII except for the η_ψ functional renormalization group value from [40].

Method and source	η_ψ	η_ϕ	$1/\nu$
Large N [32–36]	0.0152	0.894	0.970
Conformal bootstrap [28]	0.016	0.888	0.97
Four loop two-sided Padé [40]	0.0151	0.893	0.9840
Four loop interpolating polynomial [40]	0.0150	0.893	0.9763
Four loop Padé-Borel [40]	0.0120(48)	0.893(9)	0.9580(75)
Functional renormalization group [40]	0.011	0.911	0.980

TABLE VIII. Summary of previous exponent estimates for $N = 5$.

Padé	η_ψ	η_ϕ	$1/\nu$
[1/2]	——	0.906801	0.991323
[2/1]	——	0.925000	1.000000
[2/3]	——	0.899023	0.990855
[3/2]	0.016010	0.895482	0.989372
[3/4]	0.014678	0.889395	——
[4/3]	0.014680	0.891326	0.980097
[4/5]	0.015218	0.892547	0.976555
[5/4]	0.015055	0.892462	——
[5/5]	0.015070	0.892288	0.979693

TABLE IX. Two-sided Padé exponent estimates $\mathcal{P}_{[m/n]}(3)$ for $N = 5$.

Polynomial	η_ψ	η_ϕ	$1/\nu$
[1, 1]	0.009615	0.914530	0.991247
[1, 2]	0.015642	0.896196	0.991156
[2, 2]	0.013890	0.898567	0.986445
[2, 3]	0.015018	0.892908	0.980349
[3, 3]	0.014535	0.893099	0.977654
[3, 4]	0.015041	0.893362	0.977896
[4, 4]	0.015013	0.892816	0.976292
[4, 5]	0.015041	0.892008	0.980487

TABLE X. Interpolating polynomial $\mathcal{I}_{[i,j]}(3)$ exponent estimates for $N = 5$.

VI. CONCLUSIONS

One of the main aims of our study was to establish the five loop renormalization group functions of the four dimensional GNY model with a multiplet of N fermions. In achieving this level of accuracy we have been able to apply the results to improve estimates of critical exponents for phase transitions in materials such as graphene by using several summation approaches. These exploit the d-dimensional connection of the GN and GNY models that guide the ϵ expansion along a reliable path to three dimensions.

Previous lower loop results, [38–40], had shown an encouraging trend towards agreement with other methods such as the functional renormalization group technology and the conformal bootstrap approach. In the last few years improved bootstrap exponents have become available, [29, 30], so that it was necessary to move the perturbative analysis to the next loop order. The first phase of this has now been completed here with updated two-sided Padé approximant and interpolating polynomial constructions in d-dimensions. The second phase would require five loop GN renormalization group functions to fully refine the new dimension four based analysis carried out here.

In respect of that the general picture for $N = 2$ appears to be similar to the conclusions of the four loop analysis of [40] in that there is reasonable agreement with the latest bootstrap exponent estimates. For instance for η_ϕ and to a slightly lesser degree $1/\nu$ the estimates are on the edge of the uncertainty bands of [29, 30]. The situation with η_ψ is harder to pin down given that its value is small being of the magnitude of a few hundredths. Despite this our two perturbative summations, especially the interpolating polynomial one, are edging closer to the latest η_ψ conformal bootstrap value. This is an encouraging motivation to complete the five loop analysis of the universality class started here by renormalizing the GN model to the same order.

Data Availability Statement. The data that support the findings of this article are openly available [79].

ACKNOWLEDGMENTS

The work of J.A.G. was carried out with the support of the STFC Consolidated Grant ST/X000699/1 and a Visiting Scholarship from the Kolleg Mathematik Physik Berlin. The work of A.M. was supported in part by the Spanish Ministry of Science and Innovation (PID2020-112965GB-I00,PID2023-146142NB-I00), and by the Departament de Recerca i Universities from Generalitat de Catalunya to the Grup de Recerca 00649 (Codi: 2021 SGR 00649). This project received funding from the European Union's Horizon 2020 research and innovation programme under grant agreement No 824093. IFAE is partially funded by the CERCA program of the Generalitat de Catalunya. Y.S. acknowledges support from ANID/FONDECYT project No. 1231056, ANID/Exploración project No. 13250014 and UBB/VRIP project No. EQ2351247. For the purpose of open access, the authors have applied a Creative Commons Attribution (CC-BY) licence to any Author Accepted Manuscript version arising. The authors thank Igor Herbut for useful comments.

Appendix A: Large N critical exponents

In order to carry out the large N check of the exponents by comparing with those derived from the five loop results, we record the explicit expressions for the relevant large N critical exponents. These have been determined in $d = 2\mu$ dimensions in a variety of articles. For instance the fermion anomalous dimension is available to $\mathcal{O}(1/N^3)$ [31, 33, 36] being given by

$$\begin{aligned}\eta_\psi = \frac{\eta_1}{N} &+ \left(\frac{1}{2\mu} + \frac{1}{(\mu-1)^2} + \frac{1}{2(\mu-1)} + \frac{3}{(\mu-2)} + \frac{4}{(2\mu-3)} + \frac{(2\mu-1)}{(\mu-1)} \hat{\Psi}(\mu) \right) \frac{\eta_1^2}{N^2} \\
&+ \left(\frac{1}{2\mu^2} - \frac{9}{2} - \frac{7}{2\mu} - \frac{5}{4(\mu-1)^4} - \frac{3}{(\mu-1)^3} - \frac{51}{4(\mu-1)^2} - \frac{79}{4(\mu-1)} + \frac{9}{(\mu-2)^2} + \frac{153}{4(\mu-2)} + \frac{16}{(2\mu-3)^2} \right. \\
&\quad - \frac{52}{(2\mu-3)} - \mu + \left(6 + \frac{5}{4(\mu-1)^2} - \frac{3}{(\mu-1)} + \frac{12}{(\mu-2)} + \frac{27}{2(2\mu-3)} + \frac{1}{4}\mu \right) \hat{\Theta}(\mu) + \frac{3\mu^2}{(\mu-1)} \hat{\Psi}(\mu) \hat{\Theta}(\mu) \\
&\quad + \left(\frac{3}{2\mu} - \frac{3}{2} + \frac{1}{(\mu-1)^3} + \frac{2}{(\mu-1)^2} - \frac{22}{(\mu-1)} + \frac{27}{(\mu-2)} + \frac{48}{(2\mu-3)} - \mu \right) \hat{\Psi}(\mu) + \frac{3\mu^2}{2(\mu-1)} \Xi(\mu) \hat{\Theta}(\mu) \\
&\quad \left. + \frac{(2\mu-1)^2}{2(\mu-1)^2} \left(\hat{\Phi}(\mu) + 3\hat{\Psi}^2(\mu) \right) \right) \frac{\eta_1^3}{N^3} + \mathcal{O}\left(\frac{1}{N^4} \right)
\end{aligned} \tag{A1}$$

where [31, 80]

$$\eta_1 = - \frac{\Gamma(2\mu-1)}{2\mu\Gamma^2(\mu)\Gamma(\mu-1)\Gamma(1-\mu)} \, . \tag{A2}$$

The expressions for η_ψ and the remaining exponents are recorded with the four dimensional spinor trace convention for consistency although several of the original results were constructed in relation to the two dimensional GN model convention. We have introduced the shorthand notation

$$\begin{aligned}
\hat{\Psi}(\mu) &= \psi(2\mu-3) - \psi(1) + \psi(3-\mu) - \psi(\mu-1) \\
\hat{\Phi}(\mu) &= \psi'(2\mu-3) - \psi'(3-\mu) - \psi'(\mu-1) + \psi'(1) \\
\hat{\Theta}(\mu) &= \psi'(\mu-1) - \psi'(1)
\end{aligned} \tag{A3}$$

where the ϵ expansion of each function near four dimensions involves ζ_n only. At $\mathcal{O}(1/N^3)$ the function $\Xi(\mu)$ appears which is related to a specific two loop Feynman integral introduced in [81] and given in equation (4.13) of [36] in relation to the GN universality class. When $\mu = 2 - \frac{1}{2}\epsilon$ then the combination $\Xi(\mu)\hat{\Theta}(\mu)$ has the expansion

$$\begin{aligned}\Xi(\mu)\hat{\Theta}(\mu) = \frac{2}{3}\zeta_3\epsilon &+ \left(\frac{1}{3}\zeta_3 + \frac{1}{2}\zeta_4 - \frac{5}{4}\zeta_5 \right) \epsilon^2 + \left(\frac{1}{3}\zeta_5 - \frac{25}{16}\zeta_6 + \frac{1}{4}\zeta_4 + \frac{1}{6}\zeta_3 + \frac{5}{8}\zeta_3^2 \right) \epsilon^3 \\
&+ \left(\frac{5}{24}\zeta_6 - \frac{121}{64}\zeta_7 + \frac{1}{6}\zeta_5 + \frac{1}{8}\zeta_4 + \frac{1}{12}\zeta_3 + \frac{15}{16}\zeta_3\zeta_4 \right) \epsilon^4 \\
&+ \left(\frac{9}{80}\zeta_{5,3} - \frac{577}{320}\zeta_8 + \frac{1}{8}\zeta_7 + \frac{5}{48}\zeta_6 + \frac{1}{12}\zeta_5 + \frac{1}{16}\zeta_4 + \frac{1}{24}\zeta_3 + \frac{9}{8}\zeta_3\zeta_5 \right) \epsilon^5 + \mathcal{O}(\epsilon^6)
\end{aligned} \tag{A4}$$

which was deduced from the discussion given in [82, 83] and $\zeta_{5,3}$ is a multiple zeta. The critical exponent relating to the scalar field is, [34, 35],

$$\begin{aligned}\eta_\phi = 4 \; - \; 2\mu - \; & \frac{2(2\mu-1)}{(\mu-1)}\frac{\eta_1}{N} \\ & + \left(6 - \frac{1}{\mu} + \frac{5}{(\mu-1)^3} + \frac{13}{(\mu-1)^2} + \frac{29}{(\mu-1)} - \frac{18}{(\mu-2)} - \frac{32}{(2\mu-3)} + 4\mu - \frac{6\mu^2}{(\mu-1)}\hat{\Theta}(\mu) - \frac{2(2\mu-1)^2}{(\mu-1)^2}\hat{\Psi}(\mu)\right)\frac{\eta_1^2}{N^2} \\ & + \mathcal{O}\left(\frac{1}{N^3}\right) \end{aligned} \tag{A5}$$

at $\mathcal{O}(1/N^2)$ while the dimension of its mass operator is, [34, 35],

$$\begin{aligned}\eta_{\phi^2} = - \; & \frac{2\mu(2\mu-1)}{(\mu-1)}\frac{\eta_1}{N} \\ & + \left(\frac{2\mu}{(\mu-1)(\mu-2)^2\eta_1} - 38 + \frac{38}{(\mu-1)^2} + \frac{134}{(\mu-1)} + \frac{8}{(\mu-2)^3} - \frac{16}{(\mu-2)^2} - \frac{182}{(\mu-2)} - \frac{144}{(2\mu-3)} - 16\mu + 8\mu^2 \right. \\ & - \frac{3\mu^2(2\mu^2-11\mu+8)}{(\mu-1)(\mu-2)}\hat{\Theta}(\mu) - \left(38 + \frac{10}{(\mu-1)^2} + \frac{14}{(\mu-1)} + \frac{24}{(\mu-2)^2} + \frac{80}{(\mu-2)} + 8\mu + 8\mu^2\right)\hat{\Psi}(\mu) \\ & \left. - \frac{4\mu^2(2\mu-3)}{(\mu-1)(\mu-2)}\left(\hat{\Phi}(\mu) + \hat{\Psi}^2(\mu)\right)\right)\frac{\eta_1^2}{N^2} \; + \; \mathcal{O}\left(\frac{1}{N^3}\right) \; . \end{aligned} \tag{A6}$$

The remaining two exponents, $\omega_\pm$, correspond to the eigen-anomalous dimensions of the matrix of critical β-function slopes β_{ij} discussed earlier. These were computed at $\mathcal{O}(1/N^2)$ in the large N expansion in [78], where the subtlety of mixing at the large N critical point was discussed, extending the leading order expression for ω_- given in [77]. Although the d-dimensional $\mathcal{O}(1/N^2)$ exponents were given implicitly in [78] we record the full expressions here partly for future reference but also to ensure our trace conventions are consistent in checking large N results with the perturbative ϵ expansion for all exponents. We have

$$\begin{aligned}\omega_+ = 4 - 2\mu + & \frac{4(2\mu-1)(3\mu-1)}{(\mu-1)}\frac{\eta_1}{N} \\ & + \left(24 - \frac{2}{\mu} - \frac{38}{(\mu-1)^3} - \frac{394}{(\mu-1)^2} - \frac{1106}{(\mu-1)} - \frac{48}{(\mu-2)^3} + \frac{96}{(\mu-2)^2} + \frac{1056}{(\mu-2)} + \frac{800}{(2\mu-3)} - 16\mu - 192\mu^2 \right. \\ & - \frac{12\mu}{(\mu-1)(\mu-2)^2\eta_1} + \left(212 + \frac{56}{(\mu-1)^2} + \frac{68}{(\mu-1)} + \frac{144}{(\mu-2)^2} + \frac{480}{(\mu-2)} + 48\mu + 48\mu^2\right)\hat{\Psi}(\mu) \\ & \left. + \frac{54\mu^2(2\mu^2-7\mu+4)}{(\mu-1)(\mu-2)}\hat{\Theta}(\mu) + \frac{24\mu^2(2\mu-3)}{(\mu-1)(\mu-2)}\left(\hat{\Phi}(\mu) + \hat{\Psi}^2(\mu)\right)\right)\frac{\eta_1^2}{N^2} \; + \; \mathcal{O}\left(\frac{1}{N^3}\right) \end{aligned} \tag{A7}$$

and

$$\begin{aligned}\omega_- = 4 - 2\mu + & \frac{4(2\mu-1)(\mu-2)}{(\mu-1)}\frac{\eta_1}{N} \\ & + \left(88 - \frac{19}{\mu} + \frac{9}{(\mu-1)^3} + \frac{1}{(\mu-1)^2} + \frac{39}{(\mu-1)} + \frac{20}{(\mu-2)^2} + \frac{54}{(\mu-2)} - \frac{18}{(\mu-3)} - \frac{32}{(2\mu-3)} + 30\mu - 32\mu^2 + 8\mu^3 \right. \\ & - \frac{2(2\mu-3)(2\mu^3-6\mu^2+11\mu-9)}{(\mu-1)(\mu-2)(\mu-3)\eta_1} + \frac{3\mu(4\mu^3-14\mu^2+16\mu-9)}{(\mu-1)}\hat{\Theta}(\mu) \\ & \left. + \left(24 - \frac{14}{(\mu-1)} + \frac{20}{(\mu-2)} + \frac{36}{(\mu-3)} - 24\mu + 32\mu^2\right)\hat{\Psi}(\mu)\right)\frac{\eta_1^2}{N^2} \; + \; \mathcal{O}\left(\frac{1}{N^3}\right) \; . \end{aligned} \tag{A8}$$

If we expand each exponent in powers of ϵ near four dimensions and compare with the corresponding exponents from the explicit five loop computation we find total agreement to the above respective orders in $1/N$. Essential for the η_ψ check at four and five loops at $\mathcal{O}(1/N^3)$ were the $\mathcal{O}(\epsilon^3)$ and higher terms of $\Xi(\mu)\hat{\Theta}(\mu)$ in (A4). For completeness and

for future higher order computations we note the ϵ expansion for η_ψ is

$$\begin{aligned}
\eta_\psi = &\left(\frac{1}{4}\epsilon - \frac{3}{16}\epsilon^2 - \frac{3}{64}\epsilon^3 + \left(\frac{1}{16}\zeta_3 - \frac{3}{256}\right)\epsilon^4 + \left(\frac{3}{64}\zeta_4 - \frac{3}{64}\zeta_3 - \frac{3}{1024}\right)\epsilon^5 + \left(\frac{3}{64}\zeta_5 - \frac{9}{256}\zeta_4 - \frac{3}{256}\zeta_3 - \frac{3}{4096}\right)\epsilon^6\right. \\
&+ \left(\frac{1}{128}\zeta_3^2 + \frac{5}{128}\zeta_6 - \frac{9}{256}\zeta_5 - \frac{9}{1024}\zeta_4 - \frac{3}{1024}\zeta_3 - \frac{3}{16384}\right)\epsilon^7 \\
&\left.+ \left(\frac{3}{256}\zeta_3\zeta_4 + \frac{9}{256}\zeta_7 - \frac{15}{512}\zeta_6 - \frac{9}{1024}\zeta_5 - \frac{9}{4096}\zeta_4 - \frac{3}{512}\zeta_3^2 - \frac{3}{4096}\zeta_3 - \frac{3}{65536}\right)\epsilon^8\right)\frac{1}{N} \\
&+ \left(-\frac{3}{8}\epsilon + \frac{59}{64}\epsilon^2 - \frac{71}{256}\epsilon^3 - \left(\frac{25}{128} + \frac{3}{8}\zeta_3\right)\epsilon^4 + \left(\frac{91}{128}\zeta_3 - \frac{19}{256} - \frac{9}{32}\zeta_4\right)\epsilon^5\right. \\
&+ \left(\frac{273}{512}\zeta_4 - \frac{303}{16384} - \frac{73}{512}\zeta_3 - \frac{21}{64}\zeta_5\right)\epsilon^6 + \left(\frac{27}{65536} + \frac{305}{512}\zeta_5 - \frac{219}{2048}\zeta_4 - \frac{75}{256}\zeta_6 - \frac{63}{512}\zeta_3 - \frac{9}{64}\zeta_3^2\right)\epsilon^7 \\
&\left.+ \left(\frac{123}{512}\zeta_3^2 + \frac{535}{1024}\zeta_6 + \frac{631}{131072} - \frac{221}{2048}\zeta_5 - \frac{219}{4096}\zeta_3 - \frac{189}{2048}\zeta_4 - \frac{75}{256}\zeta_7 - \frac{27}{128}\zeta_3\zeta_4\right)\epsilon^8\right)\frac{1}{N^2} \\
&+ \left(\frac{9}{16}\epsilon - \frac{315}{128}\epsilon^2 + \left(\frac{527}{256} - \frac{3}{8}\zeta_3\right)\epsilon^3 + \left(\frac{665}{256}\zeta_3 + \frac{1809}{2048} - \frac{9}{32}\zeta_4\right)\epsilon^4 + \left(\frac{1995}{1024}\zeta_4 - \frac{5521}{1024}\zeta_3 - \frac{3661}{8192} - \frac{39}{128}\zeta_5\right)\epsilon^5\right. \\
&+ \left(\frac{589}{256}\zeta_5 + \frac{727}{256}\zeta_3 - \frac{16563}{4096}\zeta_4 - \frac{5817}{16384} - \frac{135}{512}\zeta_6 - \frac{105}{256}\zeta_3^2\right)\epsilon^6 \\
&+ \left(\frac{1173}{512}\zeta_3^2 + \frac{2181}{1024}\zeta_4 + \frac{2661}{2048}\zeta_3 + \frac{8455}{4096}\zeta_6 - \frac{23519}{131072} - \frac{9943}{2048}\zeta_5 - \frac{507}{2048}\zeta_7 - \frac{315}{512}\zeta_3\zeta_4\right)\epsilon^7 \\
&+ \left(\frac{27}{2560}\zeta_{5,3} + \frac{3519}{1024}\zeta_3\zeta_4 + \frac{7983}{8192}\zeta_4 + \frac{17409}{8192}\zeta_7 + \frac{20645}{8192}\zeta_5 - \frac{71825}{16384}\zeta_6 - \frac{18455}{65536}\zeta_3 - \frac{16011}{4096}\zeta_3^2 - \frac{5301}{10240}\zeta_8\right. \\
&\left.\left.\left.- \frac{2385}{32768} - \frac{315}{512}\zeta_3\zeta_5\right)\epsilon^8\right)\frac{1}{N^3} \;+\; \mathcal{O}\left(\frac{1}{N^4}\right)
\end{aligned} \tag{A9}$$

where the multiple zeta $\zeta_{5,3}$ first appears at $\mathcal{O}(\epsilon^8)$ in the third order large N term. For the remaining exponents the analogous expansions are

$$\begin{aligned}
\eta_\phi = &\,\epsilon + \left(-\frac{3}{2}\epsilon + \frac{7}{8}\epsilon^2 + \frac{11}{32}\epsilon^3 + \left(\frac{19}{128} - \frac{3}{8}\zeta_3\right)\epsilon^4 + \left(\frac{7}{32}\zeta_3 + \frac{35}{512} - \frac{9}{32}\zeta_4\right)\epsilon^5 + \left(\frac{11}{128}\zeta_3 + \frac{21}{128}\zeta_4 + \frac{67}{2048} - \frac{9}{32}\zeta_5\right)\epsilon^6\right. \\
&+ \left(\frac{19}{512}\zeta_3 + \frac{21}{128}\zeta_5 + \frac{33}{512}\zeta_4 + \frac{131}{8192} - \frac{15}{64}\zeta_6 - \frac{3}{64}\zeta_3^2\right)\epsilon^7 \\
&\left.+ \left(\frac{7}{256}\zeta_3^2 + \frac{33}{512}\zeta_5 + \frac{35}{256}\zeta_6 + \frac{35}{2048}\zeta_3 + \frac{57}{2048}\zeta_4 + \frac{259}{32768} - \frac{27}{128}\zeta_7 - \frac{9}{128}\zeta_3\zeta_4\right)\epsilon^8\right)\frac{1}{N} \\
&+ \left(\frac{9}{4}\epsilon - \frac{51}{32}\epsilon^2 - \left(\frac{281}{128} + \frac{3}{2}\zeta_3\right)\epsilon^3 + \left(\frac{9}{2}\zeta_3 + \frac{13}{64} - \frac{9}{8}\zeta_4\right)\epsilon^4 + \left(\frac{27}{8}\zeta_4 + \frac{33}{128} - \frac{159}{64}\zeta_3 - \frac{3}{4}\zeta_5\right)\epsilon^5\right. \\
&+ \left(\frac{99}{32}\zeta_5 + \frac{2127}{8192} - \frac{477}{256}\zeta_4 - \frac{363}{256}\zeta_3 - \frac{15}{32}\zeta_6 - \frac{3}{4}\zeta_3^2\right)\epsilon^6 \\
&+ \left(\frac{11}{128}\zeta_3 + \frac{63}{32}\zeta_3^2 + \frac{315}{128}\zeta_6 + \frac{7557}{32768} - \frac{1089}{1024}\zeta_4 - \frac{537}{256}\zeta_5 - \frac{9}{8}\zeta_3\zeta_4 - \frac{9}{32}\zeta_7\right)\epsilon^7 \\
&+ \left(\frac{33}{512}\zeta_4 + \frac{189}{64}\zeta_3\zeta_4 + \frac{279}{128}\zeta_7 + \frac{345}{2048}\zeta_3 + \frac{12121}{65536} - \frac{1075}{1024}\zeta_5 - \frac{945}{512}\zeta_6 - \frac{267}{256}\zeta_3^2 - \frac{21}{32}\zeta_8\right. \\
&\left.\left.\left.- \frac{15}{16}\zeta_3\zeta_5\right)\epsilon^8\right)\frac{1}{N^2} \;+\; \mathcal{O}\left(\frac{1}{N^3}\right)
\end{aligned} \tag{A10}$$

$$\begin{aligned}
\eta_{\phi^2} = &\left(-3\epsilon + \frac{5}{2}\epsilon^2 + \frac{1}{4}\epsilon^3 + \left(\frac{1}{8} - \frac{3}{4}\zeta_3\right)\epsilon^4 + \left(\frac{1}{16} + \frac{5}{8}\zeta_3 - \frac{9}{16}\zeta_4\right)\epsilon^5 + \left(\frac{1}{16}\zeta_3 + \frac{1}{32} + \frac{15}{32}\zeta_4 - \frac{9}{16}\zeta_5\right)\epsilon^6\right. \\
&+ \left(\frac{1}{32}\zeta_3 + \frac{1}{64} + \frac{3}{64}\zeta_4 + \frac{15}{32}\zeta_5 - \frac{15}{32}\zeta_6 - \frac{3}{32}\zeta_3^2\right)\epsilon^7 \\
&\left.+ \left(\frac{1}{64}\zeta_3 + \frac{1}{128} + \frac{3}{64}\zeta_5 + \frac{3}{128}\zeta_4 + \frac{5}{64}\zeta_3^2 + \frac{25}{64}\zeta_6 - \frac{27}{64}\zeta_7 - \frac{9}{64}\zeta_3\zeta_4\right)\epsilon^8\right)\frac{1}{N}
\end{aligned}$$

$$+\left(27\epsilon-\frac{147}{4}\epsilon^2+\left(\frac{15}{16}-\frac{51}{4}\zeta_3\right)\epsilon^3+\left(\frac{35}{4}\zeta_5+\frac{191}{64}+\frac{311}{8}\zeta_3-\frac{153}{16}\zeta_4\right)\epsilon^4\right.$$
$$+\left(\frac{17}{8}\zeta_3^2+\frac{175}{16}\zeta_6+\frac{439}{256}+\frac{933}{32}\zeta_4-\frac{507}{16}\zeta_3-\frac{123}{4}\zeta_5\right)\epsilon^5$$
$$+\left(\frac{19}{16}\zeta_3+\frac{51}{16}\zeta_3\zeta_4+\frac{63}{4}\zeta_7+\frac{359}{8}\zeta_5+\frac{1495}{1024}-\frac{2205}{64}\zeta_6-\frac{1521}{64}\zeta_4-\frac{183}{16}\zeta_3^2\right)\epsilon^6$$
$$+\left(\frac{57}{64}\zeta_4+\frac{137}{16}\zeta_3\zeta_5+\frac{149}{128}\zeta_3+\frac{625}{32}\zeta_3^2+\frac{4215}{4096}+\frac{4963}{256}\zeta_8+\frac{5625}{128}\zeta_6-\frac{2929}{64}\zeta_7-\frac{857}{32}\zeta_5-\frac{549}{32}\zeta_3\zeta_4\right)\epsilon^7$$
$$+\left(\frac{75}{8}\zeta_3\zeta_6+\frac{101}{96}\zeta_3^3+\frac{109}{128}\zeta_5+\frac{411}{64}\zeta_4\zeta_5+\frac{435}{512}\zeta_3+\frac{447}{512}\zeta_4+\frac{1875}{64}\zeta_3\zeta_4+\frac{4031}{192}\zeta_9+\frac{6505}{128}\zeta_7+\frac{10871}{16384}\right.$$
$$\left.\left.-\frac{29771}{512}\zeta_8-\frac{6035}{256}\zeta_6-\frac{737}{64}\zeta_3^2-\frac{121}{4}\zeta_3\zeta_5\right)\epsilon^8\right)\frac{1}{N^2}\;+\;\mathcal{O}\left(\frac{1}{N^3}\right)\;. \tag{A11}$$

Finally the two corrections to scaling exponents are

$$\omega_+=\epsilon+\left(15\epsilon-\frac{53}{4}\epsilon^2-\frac{13}{16}\epsilon^3+\left(\frac{15}{4}\zeta_3-\frac{29}{64}\right)\epsilon^4+\left(\frac{45}{16}\zeta_4-\frac{61}{256}-\frac{53}{16}\zeta_3\right)\epsilon^5+\left(\frac{45}{16}\zeta_5-\frac{159}{64}\zeta_4-\frac{125}{1024}-\frac{13}{64}\zeta_3\right)\epsilon^6\right.$$
$$+\left(\frac{15}{32}\zeta_3^2+\frac{75}{32}\zeta_6-\frac{253}{4096}-\frac{159}{64}\zeta_5-\frac{39}{256}\zeta_4-\frac{29}{256}\zeta_3\right)\epsilon^7$$
$$\left.+\left(\frac{45}{64}\zeta_3\zeta_4+\frac{135}{64}\zeta_7-\frac{509}{16384}-\frac{265}{128}\zeta_6-\frac{87}{1024}\zeta_4-\frac{61}{1024}\zeta_3-\frac{53}{128}\zeta_3^2-\frac{39}{256}\zeta_5\right)\epsilon^8\right)\frac{1}{N}$$
$$+\left(-\frac{315}{2}\epsilon+\frac{1845}{16}\epsilon^2+\left(\frac{207}{2}\zeta_3+\frac{8767}{64}\right)\epsilon^3+\left(\frac{621}{8}\zeta_4-\frac{1113}{4}\zeta_3-\frac{105}{2}\zeta_5-49\right)\epsilon^4\right.$$
$$+\left(\frac{4965}{32}\zeta_3+198\zeta_5-\frac{3339}{16}\zeta_4-\frac{1347}{128}-\frac{525}{8}\zeta_6-\frac{51}{4}\zeta_3^2\right)\epsilon^5$$
$$+\left(\frac{657}{8}\zeta_3^2+\frac{6885}{32}\zeta_6+\frac{8325}{128}\zeta_3+\frac{14895}{128}\zeta_4-\frac{44505}{4096}-\frac{4641}{16}\zeta_5-\frac{189}{2}\zeta_7-\frac{153}{8}\zeta_3\zeta_4\right)\epsilon^6$$
$$+\left(\frac{1971}{16}\zeta_3\zeta_4+\frac{8949}{32}\zeta_7+\frac{16479}{128}\zeta_5+\frac{24975}{512}\zeta_4-\frac{139683}{16384}-\frac{14889}{128}\zeta_8-\frac{2205}{8}\zeta_6-\frac{561}{4}\zeta_3^2\right.$$
$$\left.-\frac{411}{8}\zeta_3\zeta_5-\frac{349}{16}\zeta_3\right)\epsilon^7$$
$$+\left(\frac{1587}{8}\zeta_3\zeta_5+\frac{8289}{128}\zeta_3^2+\frac{24917}{512}\zeta_5+\frac{28785}{256}\zeta_6+\frac{92337}{256}\zeta_8-\frac{195131}{32768}-\frac{4971}{16}\zeta_7-\frac{4875}{1024}\zeta_3-\frac{4031}{32}\zeta_9\right.$$
$$\left.\left.-\frac{1683}{8}\zeta_3\zeta_4-\frac{1233}{32}\zeta_4\zeta_5-\frac{1047}{64}\zeta_4-\frac{225}{4}\zeta_3\zeta_6-\frac{101}{16}\zeta_3^3\right)\epsilon^8\right)\frac{1}{N^2}\;+\;\mathcal{O}\left(\frac{1}{N^3}\right) \tag{A12}$$

and

$$\omega_-=\epsilon+\left(-\frac{3}{2}\epsilon^2+\frac{7}{8}\epsilon^3+\frac{11}{32}\epsilon^4+\left(\frac{19}{128}-\frac{3}{8}\zeta_3\right)\epsilon^5+\left(\frac{7}{32}\zeta_3+\frac{35}{512}-\frac{9}{32}\zeta_4\right)\epsilon^6\right.$$
$$\left.+\left(\frac{11}{128}\zeta_3+\frac{21}{128}\zeta_4+\frac{67}{2048}-\frac{9}{32}\zeta_5\right)\epsilon^7+\left(\frac{19}{512}\zeta_3+\frac{21}{128}\zeta_5+\frac{33}{512}\zeta_4+\frac{131}{8192}-\frac{15}{64}\zeta_6-\frac{3}{64}\zeta_3^2\right)\epsilon^8\right)\frac{1}{N}$$
$$+\left(\frac{87}{32}\epsilon^2+\left(\frac{27}{8}\zeta_3-\frac{293}{128}\right)\epsilon^3+\left(\frac{81}{32}\zeta_4-\frac{419}{128}-\frac{375}{32}\zeta_3\right)\epsilon^4+\left(\frac{13}{4}\zeta_5+\frac{1945}{1024}+\frac{2059}{128}\zeta_3-\frac{1125}{128}\zeta_4\right)\epsilon^5\right.$$
$$+\left(\frac{49}{32}\zeta_3^2+\frac{385}{128}\zeta_6+\frac{6177}{512}\zeta_4-\frac{4293}{512}\zeta_3-\frac{2139}{8192}-\frac{165}{16}\zeta_5\right)\epsilon^6$$
$$+\left(\frac{147}{64}\zeta_3\zeta_4+\frac{401}{128}\zeta_7+\frac{3425}{256}\zeta_5+\frac{24045}{32768}-\frac{12879}{2048}\zeta_4-\frac{4725}{512}\zeta_6-\frac{2211}{2048}\zeta_3-\frac{693}{128}\zeta_3^2\right)\epsilon^7$$
$$+\left(\frac{85}{32}\zeta_3\zeta_5+\frac{3701}{512}\zeta_3^2+\frac{4137}{1024}\zeta_8+\frac{9177}{8192}\zeta_3+\frac{23955}{2048}\zeta_6-\frac{7059}{1024}\zeta_5-\frac{6633}{8192}\zeta_4-\frac{4773}{512}\zeta_7-\frac{2079}{256}\zeta_3\zeta_4\right.$$
$$\left.\left.-\frac{955}{65536}\right)\epsilon^8\right)\frac{1}{N^2}\;+\;\mathcal{O}\left(\frac{1}{N^3}\right) \tag{A13}$$

where the $\mathcal{O}(\epsilon^4)$ terms of $\omega_\pm$ were provided in [78]. We note that the leading terms of both $\omega_\pm$ are the same unlike their $N = 2$ perturbative counterparts in (28) and (29). This is because while the leading ϵ term of (28) is solely ϵ the coefficient of the corresponding term (29) is N dependent being in particular $\frac{\sqrt{(4N^2+132N+9)}}{(2N+3)}$ as can be seen in [17] after adjusting for the different N convention. Clearly this tends to unity as $N \to \infty$.

Appendix B: Gross-Neveu model critical exponents

For completeness we record the four loop $O(N)$ GN critical exponents here in the same conventions as the GNY theory. From [37] we have

$$\begin{aligned}
\eta_\psi &= \frac{(4N-1)}{8(2N-1)^2}\epsilon^2 \;-\; \frac{(2N-3)(4N-1)}{16(2N-1)^3}\epsilon^3 \;+\; \frac{(4N-1)(16N^2-44N+25)}{128(2N-1)^4}\epsilon^4 \;+\; \mathcal{O}(\epsilon^5) \\
\eta_\phi &= 2 \;-\; \frac{2N}{(2N-1)}\epsilon \;-\; \frac{(4N-1)}{4(2N-1)^2}\epsilon^2 \;+\; \frac{N(4N-1)}{4(2N-1)^3}\epsilon^3 \\
&\quad + \frac{(4N-1)(4(8N^2+14N-21)\zeta_3 - 16N^2+36N+5)}{64(2N-1)^4}\epsilon^4 \;+\; \mathcal{O}(\epsilon^5) \\
\frac{1}{\nu} &= \epsilon \;-\; \frac{1}{2(2N-1)}\epsilon^2 \;-\; \frac{(4N-3)}{8(2N-1)^2}\epsilon^3 \;+\; \frac{((4N-1)(N+3)+3(22N-17)\zeta_3)}{8(2N-1)^3}\epsilon^4 \;+\; \mathcal{O}(\epsilon^5)
\end{aligned} \tag{B1}$$

in $d = 2 + \epsilon$ dimensions. Numerically for $N = 2$ these equate to

$$\begin{aligned}
\eta_\psi &= 0.097222\epsilon^2 \;-\; 0.016204\epsilon^3 \;+\; 0.000675\epsilon^4 \;+\; \mathcal{O}(\epsilon^5) \\
\eta_\phi &= 2.000000 \;-\; 1.333333\epsilon \;-\; 0.194444\epsilon^2 \;+\; 0.129630\epsilon^3 \;+\; 0.270765\epsilon^4 \;+\; \mathcal{O}(\epsilon^5) \\
\frac{1}{\nu} &= 1.000000\epsilon \;-\; 0.166667\epsilon^2 \;-\; 0.069444\epsilon^3 \;+\; 0.612808\epsilon^4 \;+\; \mathcal{O}(\epsilon^5) \; .
\end{aligned} \tag{B2}$$

The situation for η_ϕ and $1/\nu$ is the same as their four dimensional counterparts in that the coefficients of the higher order terms in ϵ are not decreasing in contrast to η_ψ.

[1] K. G. Wilson and J. B. Kogut, The Renormalization group and the epsilon expansion, Phys. Rept. **12**, 75 (1974).
[2] D. Poland and D. Simmons-Duffin, The conformal bootstrap, Nature Phys. **12**, 535 (2016).
[3] J. Henriksson, The critical O(N) CFT: Methods and conformal data, Phys. Rept. **1002**, 1 (2023), arXiv:2201.09520 [hep-th].
[4] K. G. Wilson, Feynman graph expansion for critical exponents, Phys. Rev. Lett. **28**, 548 (1972).
[5] H. Kleinert, J. Neu, V. Schulte-Frohlinde, K. G. Chetyrkin, and S. A. Larin, Five loop renormalization group functions of $O(n)$ symmetric ϕ^4 theory and epsilon expansions of critical exponents up to ϵ^5, Phys. Lett. B **272**, 39 (1991), [Erratum: Phys. Lett. B 319, 545 (1993)], arXiv:hep-th/9503230.
[6] M. V. Kompaniets and E. Panzer, Minimally subtracted six loop renormalization of $O(n)$-symmetric ϕ^4 theory and critical exponents, Phys. Rev. D **96**, 036016 (2017), arXiv:1705.06483 [hep-th].
[7] O. Schnetz, Numbers and Functions in Quantum Field Theory, Phys. Rev. D **97**, 085018 (2018), arXiv:1606.08598 [hep-th].
[8] D. J. Gross and A. Neveu, Dynamical Symmetry Breaking in Asymptotically Free Field Theories, Phys. Rev. D **10**, 3235 (1974).
[9] J. Zinn-Justin, Four fermion interaction near four-dimensions, Nucl. Phys. B **367**, 105 (1991).
[10] L. Balents, M. P. A. Fisher, and C. Nayak, Nodal Liquid Theory of the Pseudo-Gap Phase of High-T_c Superconductors, Int. J. Mod. Phys. B **12**, 1033 (1998), arXiv:cond-mat/9803086.
[11] S.-S. Lee, Emergence of supersymmetry at a critical point of a lattice model, Phys. Rev. B **76**, 075103 (2007), arXiv:cond-mat/0611658.
[12] P. Ponte and S.-S. Lee, Emergence of supersymmetry on the surface of three dimensional topological insulators, New J. Phys. **16**, 013044 (2014), arXiv:1206.2340 [cond-mat.str-el].
[13] T. Grover, D. N. Sheng, and A. Vishwanath, Emergent Space-Time Supersymmetry at the Boundary of a Topological Phase, Science **344**, 280 (2014), arXiv:1301.7449 [cond-mat.str-el].
[14] L. Fei, S. Giombi, I. R. Klebanov, and G. Tarnopolsky, Yukawa CFTs and Emergent Supersymmetry, PTEP **2016**, 12C105 (2016), arXiv:1607.05316 [hep-th].
[15] I. F. Herbut, Interactions and phase transitions on graphene's honeycomb lattice, Phys. Rev. Lett. **97**, 146401 (2006), arXiv:cond-mat/0606195.
[16] I. F. Herbut, V. Juričić, and O. Vafek, Relativistic Mott criticality in graphene, Phys. Rev. B **80**, 075432 (2009), arXiv:0904.1019 [cond-mat.str-el].

[17] L. Kärkkäinen, R. Lacaze, P. Lacock, and B. Petersson, Critical behavior of the three-dimensional Gross-Neveu and Higgs-Yukawa models, Nucl. Phys. B **415**, 781 (1994), [Erratum: Nucl. Phys. B 438, 650–650 (1995)], arXiv:hep-lat/9310020.

[18] S. Chandrasekharan and A. Li, Quantum critical behavior in three dimensional lattice Gross-Neveu models, Phys. Rev. D **88**, 021701 (2013), arXiv:1304.7761 [hep-lat].

[19] Z.-X. Li, Y.-F. Jiang, and H. Yao, Fermion-sign-free Majarana-quantum-Monte-Carlo studies of quantum critical phenomena of Dirac fermions in two dimensions, New J. Phys. **17**, 085003 (2015), arXiv:1411.7383 [cond-mat.str-el].

[20] Y.-Y. He, X. Y. Xu, K. Sun, F. F. Assaad, Z. Y. Meng, and Z.-Y. Lu, Dynamical Generation of Topological Masses in Dirac Fermions, Phys. Rev. B **97**, 081110 (2018), arXiv:1705.09192 [cond-mat.str-el].

[21] E. Huffman and S. Chandrasekharan, Fermion bag approach to Hamiltonian lattice field theories in continuous time, Phys. Rev. D **96**, 114502 (2017), arXiv:1709.03578 [hep-lat].

[22] Y. Liu, W. Wang, K. Sun, and Z. Y. Meng, Designer Monte Carlo simulation for the Gross-Neveu-Yukawa transition, Phys. Rev. B **101**, 064308 (2020), arXiv:1910.07430 [cond-mat.stat-mech].

[23] E. Huffman and S. Chandrasekharan, Fermion-bag inspired Hamiltonian lattice field theory for fermionic quantum criticality, Phys. Rev. D **101**, 074501 (2020), arXiv:1912.12823 [cond-mat.str-el].

[24] T.-T. Wang and Z. Y. Meng, Quantum Monte Carlo calculation of critical exponents of the Gross-Neveu-Yukawa on a two-dimensional fermion lattice model, Phys. Rev. B **108**, L121112 (2023), arXiv:2304.00034 [cond-mat.str-el].

[25] L. Janssen and I. F. Herbut, Antiferromagnetic critical point on graphene's honeycomb lattice: A functional renormalization group approach, Phys. Rev. B **89**, 205403 (2014), [Erratum: Phys. Rev. B 102, 199902 (2020)], arXiv:1402.6277 [cond-mat.str-el].

[26] B. Knorr, Ising and Gross-Neveu model in next-to-leading order, Phys. Rev. B **94**, 245102 (2016), arXiv:1609.03824 [cond-mat.str-el].

[27] B. Hawashin, M. M. Scherer, M. Smolkin, and L. Yung, Spontaneous Space-Time Parity Breaking Without Thermal Restoration (2025), arXiv:2507.19890 [hep-th].

[28] L. Iliesiu, F. Kos, D. Poland, S. S. Pufu, and D. Simmons-Duffin, Bootstrapping 3D Fermions with Global Symmetries, J. High Energy Phys. **01**, 036 (2018), arXiv:1705.03484 [hep-th].

[29] R. S. Erramilli, L. V. Iliesiu, P. Kravchuk, A. Liu, D. Poland, and D. Simmons-Duffin, The Gross-Neveu-Yukawa archipelago, J. High Energy Phys. **02**, 036 (2023), arXiv:2210.02492 [hep-th].

[30] M. S. Mitchell and D. Poland, Bounding irrelevant operators in the 3d Gross-Neveu-Yukawa CFTs, J. High Energy Phys. **09**, 134 (2024), arXiv:2406.12974 [hep-th].

[31] J. A. Gracey, Calculation of exponent η to $O(1/N^2)$ in the $O(N)$ Gross-Neveu model, Int. J. Mod. Phys. A **6**, 395 (1991), [Erratum: Int. J. Mod. Phys.A 6, 2755 (1991)].

[32] J. A. Gracey, Anomalous mass dimension at $O(1/N^2)$ in the $O(N)$ Gross-Neveu model, Phys. Lett. B **297**, 293 (1992).

[33] A. N. Vasiliev, S. E. Derkachov, N. A. Kivel, and A. S. Stepanenko, The $1/n$ expansion in the Gross-Neveu model: Conformal bootstrap calculation of the index η in order $1/n^3$, Theor. Math. Phys. **94**, 127 (1993).

[34] A. N. Vasiliev and A. S. Stepanenko, The $1/n$ expansion in the Gross-Neveu model: Conformal bootstrap calculation of the exponent $1/\nu$ to the order $1/n^2$, Theor. Math. Phys. **97**, 1349 (1993).

[35] J. A. Gracey, Computation of $\beta'(g_c)$ at $O(1/N^2)$ in the $O(N)$ Gross-Neveu model in arbitrary dimensions, Int. J. Mod. Phys. A **9**, 567 (1994), arXiv:hep-th/9306106.

[36] J. A. Gracey, Computation of critical exponent η at $O(1/N^3)$ in the four Fermi model in arbitrary dimensions, Int. J. Mod. Phys. A **9**, 727 (1994), arXiv:hep-th/9306107.

[37] J. A. Gracey, T. Luthe, and Y. Schröder, Four loop renormalization of the Gross-Neveu model, Phys. Rev. D **94**, 125028 (2016), arXiv:1609.05071 [hep-th].

[38] L. N. Mihaila, N. Zerf, B. Ihrig, I. F. Herbut, and M. M. Scherer, Gross-Neveu-Yukawa model at three loops and Ising critical behavior of Dirac systems, Phys. Rev. B **96**, 165133 (2017), arXiv:1703.08801 [cond-mat.str-el].

[39] N. Zerf, L. N. Mihaila, P. Marquard, I. F. Herbut, and M. M. Scherer, Four-loop critical exponents for the Gross-Neveu-Yukawa models, Phys. Rev. D **96**, 096010 (2017), arXiv:1709.05057 [hep-th].

[40] B. Ihrig, L. N. Mihaila, and M. M. Scherer, Critical behavior of Dirac fermions from perturbative renormalization, Phys. Rev. B **98**, 125109 (2018), arXiv:1806.04977 [cond-mat.str-el].

[41] B. Rosenstein, H.-L. Yu, and A. Kovner, Critical exponents of new universality classes, Phys. Lett. B **314**, 381 (1993).

[42] T. Steudtner, Four Loop Renormalisation Group Equations in general Gross-Neveu-Yukawa Theories (2025), arXiv:2507.18710 [hep-th].

[43] W. Wetzel, Two-loop β-function for the Gross-Neveu Model, Phys. Lett. B **153**, 297 (1985).

[44] A. W. W. Ludwig, Critical behavior of the two-dimensional random q-state Potts model by expansion in $(q-2)$, Nucl. Phys. B **285**, 97 (1987).

[45] J. A. Gracey, Three loop calculations in the $O(N)$ Gross-Neveu model, Nucl. Phys. B **341**, 403 (1990).

[46] C. Luperini and P. Rossi, Three-loop β-function(s) and effective potential in the Gross-Neveu model, Annals Phys. **212**, 371 (1991).

[47] J. A. Gracey, Computation of the three-loop β-function of the $O(N)$ Gross-Neveu model in minimal subtraction, Nucl. Phys. B **367**, 657 (1991).

[48] P. Nogueira, Automatic Feynman Graph Generation, J. Comput. Phys. **105**, 279 (1993).

[49] M. Misiak and M. Münz, Two loop mixing of dimension five flavor changing operators, Phys. Lett. B **344**, 308 (1995), arXiv:hep-ph/9409454.

[50] T. van Ritbergen, J. A. M. Vermaseren, and S. A. Larin, The four-loop β-function in quantum chromodynamics, Phys. Lett. B **400**, 379 (1997), arXiv:hep-ph/9701390.

[51] K. G. Chetyrkin, M. Misiak, and M. Münz, β functions and anomalous dimensions up to three loops, Nucl. Phys. B **518**, 473 (1998), arXiv:hep-ph/9711266.
[52] J. A. M. Vermaseren, New features of FORM (2000), arXiv:math-ph/0010025.
[53] M. Tentyukov and J. A. M. Vermaseren, The Multithreaded version of FORM, Comput. Phys. Commun. **181**, 1419 (2010), arXiv:hep-ph/0702279.
[54] A. Maier, `https://github.com/a-maier/dynast`.
[55] B. D. McKay and A. Piperno, Practical graph isomorphism, ii, J. Symb. Comput. **60**, 94 (2014), arXiv:1301.1493 [cs.DM].
[56] S. Laporta, High precision calculation of multiloop Feynman integrals by difference equations, Int. J. Mod. Phys. **A15**, 5087 (2000), arXiv:hep-ph/0102033 [hep-ph].
[57] P. Marquard and D. Seidel, The IBP package `Crusher`, unpublished.
[58] A. Maier and P. Marquard, `tinbox`, a finite field solver, unpublished.
[59] K. G. Chetyrkin and F. V. Tkachov, Integration by parts: The algorithm to calculate β-functions in 4 loops, Nucl. Phys. B **192**, 159 (1981).
[60] F. V. Tkachov, A theorem on analytical calculability of 4-loop renormalization group functions, Phys. Lett. B **100**, 65 (1981).
[61] M. Kauers, Fast solvers for dense linear systems, Nucl. Phys. B Proc. Suppl. **183**, 245 (2008).
[62] P. Kant, Finding linear dependencies in integration-by-parts equations: A Monte Carlo approach, Comput. Phys. Commun. **185**, 1473 (2014), arXiv:1309.7287 [hep-ph].
[63] A. von Manteuffel and R. M. Schabinger, A novel approach to integration by parts reduction, Phys. Lett. B **744**, 101 (2015), arXiv:1406.4513 [hep-ph].
[64] T. Peraro, Scattering amplitudes over finite fields and multivariate functional reconstruction, J. High Energy Phys. **12**, 030 (2016), arXiv:1608.01902 [hep-ph].
[65] J. Klappert and F. Lange, Reconstructing rational functions with FireFly, Comput. Phys. Commun. **247**, 106951 (2020), arXiv:1904.00009 [cs.SC].
[66] T. Luthe, Fully massive vacuum integrals at 5 loops, Ph.D. thesis, Bielefeld University (2015).
[67] T. Luthe and Y. Schröder, Fun with higher-loop Feynman diagrams, J. Phys. Conf. Ser. **762**, 012066 (2016), arXiv:1604.01262 [hep-ph].
[68] T. Luthe and Y. Schröder, Five-loop massive tadpoles, PoS **LL2016**, 074 (2016), arXiv:1609.06786 [hep-ph].
[69] R. Lewis, Fermat: A computer algebra system for polynomial and matrix computation.
[70] T. Luthe, A. Maier, P. Marquard, and Y. Schröder, Towards the five-loop Beta function for a general gauge group, J. High Energy Phys. **07**, 127 (2016), arXiv:1606.08662 [hep-ph].
[71] T. Luthe, A. Maier, P. Marquard, and Y. Schröder, Five-loop quark mass and field anomalous dimensions for a general gauge group, J. High Energy Phys. **01**, 081 (2017), arXiv:1612.05512 [hep-ph].
[72] T. Luthe, A. Maier, P. Marquard, and Y. Schröder, Complete renormalization of QCD at five loops, J. High Energy Phys. **03**, 020 (2017), arXiv:1701.07068 [hep-ph].
[73] T. Luthe, A. Maier, P. Marquard, and Y. Schröder, The five-loop Beta function for a general gauge group and anomalous dimensions beyond Feynman gauge, J. High Energy Phys. **10**, 166 (2017), arXiv:1709.07718 [hep-ph].
[74] H. R. P. Ferguson, D. H. Bailey, and S. Arno, Analysis of PSLQ, an integer relation finding algorithm, Math. Comput. **68**, 351 (1999).
[75] F. M. Dittes, Y. A. Kubyshin, and O. V. Tarasov, Four Loop Approximation in the ϕ^4 Model, Theor. Math. Phys. **37**, 879 (1978).
[76] S. G. Gorishnii, S. A. Larin, F. V. Tkachov, and K. G. Chetyrkin, Five-loop renormalization group calculations in the $g\phi^4$ in theory, Phys. Lett. B **132**, 351 (1983).
[77] J. A. Gracey, Critical exponent ω in the Gross-Neveu-Yukawa model at $O(1/N)$, Phys. Rev. D **96**, 065015 (2017), arXiv:1707.05275 [hep-th].
[78] A. N. Manashov and M. Strohmaier, Correction exponents in the Gross–Neveu–Yukawa model at $1/N^2$, Eur. Phys. J. C **78**, 454 (2018), arXiv:1711.02493 [hep-th].
[79] J. Gracey, A. Maier, P. Marquard, and Y. Schröder, Data representing the main results recorded here are available from the arXiv version of this article (2025).
[80] S. Hands, A. Kocić, and J. B. Kogut, Four Fermi theories in fewer than four-dimensions, Annals Phys. **224**, 29 (1993), arXiv:hep-lat/9208022.
[81] A. N. Vasiliev, Y. M. Pis'mak, and J. R. Honkonen, $1/N$ expansion: calculation of the exponent η in the order $1/N^3$ by the conformal bootstrap mathod, Theor. Math. Phys. **50**, 127 (1982).
[82] D. J. Broadhurst, J. A. Gracey, and D. Kreimer, Beyond the triangle and uniqueness relations: Nonzeta counterterms at large N from positive knots, Z. Phys. C **75**, 559 (1997), arXiv:hep-th/9607174.
[83] D. J. Broadhurst and A. V. Kotikov, Compact analytical form for nonzeta terms in critical exponents at order $1/N^3$, Phys. Lett. B **441**, 345 (1998), arXiv:hep-th/9612013.